EFFECT OF ZN ADDITIONS ON THE ELECTROCHEMICAL MIGRATION BEHAVIOUR OF SAC305 SOLDER ALLOYS

LOH HWEI LING

FACULTY OF ENGINEERING
UNIVERSITY OF MALAYA
KUALA LUMPUR

2019

University of Malaya

EFFECT OF ZN ADDITIONS ON THE ELECTROCHEMICAL MIGRATION BEHAVIOUR OF SAC305 SOLDER ALLOYS

LOH HWEI LING

RESEARCH PROJECT SUBMITTED IN PARTIAL FULFILMENT OF THE REQUIREMENTS FOR THE DEGREE OF MASTERS OF MATERIALS ENGINEERING

FACULTY OF ENGINEERING
UNIVERSITY OF MALAYA
KUALA LUMPUR

2019

University of Malaya

UNIVERSITY OF MALAYA

ORIGINAL LITERARY WORK DECLARATION

Name of Candidate: **LOH HWEI LING**

Matric No:

Name of Degree: **MASTERS OF MATERIALS ENGINEERING**

Title of Project Paper/Research Report/Dissertation/Thesis ("this Work"):

EFFECT OF ZN ADDITIONS ON THE ELECTROCHEMICAL MIGRATION BEHAVIOUR OF SAC305 SOLDER ALLOYS

Field of Study: Masters of Materials Engineering

I do solemnly and sincerely declare that:

(1) I am the sole author/writer of this Work;
(2) This Work is original;
(3) Any use of any work in which copyright exists was done by way of fair dealing and for permitted purposes and any excerpt or extract from, or reference to or reproduction of any copyright work has been disclosed expressly and sufficiently and the title of the Work and its authorship have been acknowledged in this Work;
(4) I do not have any actual knowledge nor do I ought reasonably to know that the making of this work constitutes an infringement of any copyright work;
(5) I hereby assign all and every rights in the copyright to this Work to the University of Malaya ("UM"), who henceforth shall be owner of the copyright in this Work and that any reproduction or use in any form or by any means whatsoever is prohibited without the written consent of UM having been first had and obtained;
(6) I am fully aware that if in the course of making this Work I have infringed any copyright whether intentionally or otherwise, I may be subject to legal action or any other action as may be determined by UM.

Candidate's Signature   Date:

Subscribed and solemnly declared before,

Witness's Signature   Date:

Name:

Designation:

University of Malaya

EFFECT OF ZN ADDITIONS ON THE ELECTROCHEMICAL MIGRATION BEHAVIOUR OF SAC305 SOLDER ALLOYS

ABSTRACT

The inclusion of lead within the European Union's Restriction of Hazardous Substances list has led to a push within the microelectronics industry for a suitable non-lead solder alloy substitute with comparable mechanical and chemical properties. Tin-silver-copper (Sn-Ag-Cu) alloys with the addition of zinc (Zn) offers comparable performance in terms of mechanical properties but was found to be lacking in terms of corrosion resistance. In this study, the effect of zinc addition on one aspect of corrosion i.e. electrochemical migration was investigated in 1 wt% of sodium chloride solution with SAC305 as a substrate. The electrochemical migration behavior of these alloys was studied through a water drop test to observe the time-to-failure of the circuit and the subsequent test products studied under scanning electron microscopy (SEM). The water drop test results indicated that the addition of Zn would increase the time-to-failure due to the formation of intermetallic compounds at the surface of the substrate. The addition of Zn also changed the SAC305 dendritic morphology from a fern-like, thick, angular shape to a thinner, more needle-like structure.

Keywords: Electrochemical migration, lead-free solders, SAC

University of Malaya

KESAN PENAMBAHAN ZN KEPADA PENGHIJRAHAN ELEKTROKIMIA PATERI ALOI SAC305

ABSTRAK

Penyertaan plumbum dalam senarai Sekatan Bahan Berbahaya Kesatuan Eropah telah mendorong industri mikroelektronik untuk mengganti aloi pateri jenis plumbum dengan jenis yang tidak mengandungi plumbum yang mempunyai sifat mekanikal dan kimia yang setaraf dengan aloi plumbum. Aloi jenis timah-perak-tembaga (Sn-Ag-Cu) dengan penambahan zink (Zn) menawarkan prestasi yang setanding dari segi sifat mekanikal tetapi didapati kekurangan dari sifat fenomena karat. Dalam kajian ini, kesan penambahan zink kepada penghijrahan electrokimia disiasat dengan menggunakan aloi SAC305 sebagai substrat dan larutan natrium klorida 1%. Sifat-sifat penghijrahan kimia telah dikaji melalui ujian titisan air ("water drop test") dan "scanning electron microscopy". Keputusan ujian titisan air menunjukkan bahawa penambahan Zn ke dalam aloi SAC305 akan meningkatkan masa yang diambil untuk litar pintas dan gagal. Ini diakibatkan oleh pembentukan sebatian intermetal di atas permukaan SAC305 semasa ujian tersebut dijalankan. Penambahan Zn juga diperhatikan untuk mengubah morfologi dendrit SAC305 daripada jenis yang bersudut dan tebal seperti paku pakis, kepada struktur yang lebih nipis dan berjarum.

Kata kunci: Penghijrahan elektrokimia, pateri bebas plumbum, SAC

.

University of Malaya

ACKNOWLEDGEMENTS

I would like to take this opportunity to record my highest and deepest thanks to those who have supported me during my journey through my masters degree over the past few years. Without them, I would not have been able to complete this uncumbered.

My heartfelt thanks to Prof Dr. A.S. Md Abd Haseeb for his patience and continuous guidance throughout the entire process of this research. He was very knowledgable, and his guidance allowed me to achieve this work that I have today.

I would also like to extend my greatest thanks to the PhD students Lee Ee Lynn and Goh Yi Sing who were with me every step of the way. Their help and guidance from the first day of me on this project was always assuring and reliable, and I am deeply appreciative of them taking the time and effort to guide me, even on non-weekdays.

I would also like to record my sincere thanks to the faculty of engineering of Universiti Malaya as well, for allowing me use of their facilities and for being patient with all my numerous enquiries. Also, I cannot underscore the support afforded by my manager Eunice Ho who has been supportive and understanding in letting me juggle between my work and study responsibilities.

And lastly, but most importantly, a million thanks to those of my family who never stopped encouraging me throughout my entire trek in this degree. I would (literally) not be where I am today without them.

University of Malaya

Table of Contents

Abstract i

Abstrak ii

ACKNOWLEDGEMENTS iii

LIST OF FIGURES vi

LIST OF TABLES vii

List of Symbols and Abbreviations viii

1.0 INTRODUCTION 1

1.1 Study background 1

1.2 Study objectives 3

1.3 Scope of the study 3

2.0 LITERATURE REVIEW 4

2.1 Introduction 4

2.2 Physical performance characteristics of lead-free Sn-based solders 5

2.2.1 Performance comparison between SAC105 and SAC305 7

2.2.2 Influence of element addition on Sn-rich alloys 8

2.3 Chemical properties of solder alloys 10

2.3.1 The electrochemical migration (ECM) process 10

2.3.2 Electrochemical migration tests 12

2.3.3 ECM corrosion mechanisms of SAC alloys 16

2.3.4 Influence of element addition on the ECM performance of Sn-rich alloys 22

2.4 Summary and conclusion 24

3.0 RESEARCH METHODOLOGY 25

3.1 Introduction 25

3.2 Sample and solution preparation 27

3.2.1 Sample preparation 27

3.2.2 Electrolyte solution preparation 28

3.3 Electrochemical migration test 28

3.3.1 Water drop test 28

3.4 Surface characterisation test 29

3.4.1 Scanning Electron Microscopy (SEM) 29

4.0 RESULTS 30

4.1 Water drop test 30

4.2 Scanning Electron Microscopy 31

4.2.1 400x magnification 31

4.2.2 10,000x magnification 33

5.0 DISCUSSION 34

5.1 Water drop test 34

University of Malaya

5.1.1 Time-to-failure 34
5.1.2 Hydrogen gas generation.. 35
5.2 Morphological analysis of ECM corrosion products 39
6.0 CONCLUSIONS AND RECOMMENDATIONS 44
6.1 Conclusions 44
6.2 Recommendations for future works 44
REFERENCES... 46

University of Malaya

LIST OF FIGURES

Figure 2.1: Dendrite formation bridging the gap between the anode and cathode (He et al., 2014) 12

Figure 2.2: (a) Water drop test setup; (b) Optical graph of test setup at the beginning of a WD test experiment (Zhong, Yu, et al., 2017) 14

Figure 2.3: Schematic for thin electrolyte layer test: (1) 3D microscope, (2) thin electrolyte layer, (3) electrode, (4) horizontal stage, (5) glass chamber, (6) potentiostat (Zhong, Guo, et al., 2013) 15

Figure 2.4: SEM image of SAC305 alloy dendrites after 70h ECM test in 3.5 wt% NaCl solution(L Hua & Yang, 2011) 21

Figure 2.5: SEM of dendrite morphologies of SAC305 in 3.5 wt% NaCl (a, without metal doping; b, with added Zn) (L Hua et al., 2010) 23

Figure 3.1: Flowchart of experimental procedure 26

Figure 3.2: (a) Sample dimensions; (b) Full assembled system 28

Figure 4.1: Average current readings for Zn and non-Zn containing samples for water drop test 30

Figure 4.2: SE micrographs for SAC305 samples at 3000x magnification containing: (a) 0% Zn; (b) 0.1% Zn; (c) 0.3% Zn; (d) 0.5% Zn 32

Figure 4.3: SEM micrograph at 10,000x magnification of SAC305 alloy dendrites with addition of: (a) 0% Zn; (b) 0.1% Zn; (c) 0.5% Zn 33

Figure 5.0.1: Comparison of time-to-failure of SAC305 alloy solders with incremental zinc content 34

Figure 5.0.2: Effervescence formation observed at the 1 min mark for SAC305 alloys containing: (a) 0% Zn; (b) 0.1% Zn; (c) 0.3% Zn; (d) 0.5% Zn 37

Figure 5.0.3: Effervescence formation observed at the 6 min mark for SAC305 alloys containing: (a) 0% Zn; (b) 0.1% Zn; (c) 0.3% Zn; (d) 0.5% Zn 39

University of Malaya

Figure 5.0.4: Comparison of sample surface at 400x magnification of SAC305 samples containing: (a) 0% Zn; (b) 0.1% Zn; (c) 0.3% Zn; (d) 0.5% Zn 40

Figure 5.0.5: SE micrographs of the dendrite topography for SAC305 (left side) and SAC305 + 0.5% Zn (right side) at: 2000x magnification 41

Figure 5.0.6: SE micrographs of dendrite morphology at 10,000x magnifictation for: (a) SAC305; (b) SAC305 + 0.1% Zn; (c) SAC305 + 0.5% Zn 42

Figure 5.0.7: Macrostructure of dendrites for SAC alloys containing: (a) 0% Zn; (b) 0.1% Zn; (c) 0.5% Zn... 43

LIST OF TABLES

Table 2.1: Comparison of performance characteristics of commonly used solder alloys 6

Table 2.2: Comparison of performance characteristics of SAC105 and SAC305 7

Table 2.3: Comparison of performance characteristics for additional alloying element in Sn-alloys 9

Table 2.4: Comparison of ECM corrosion test methods 13

Table 2.5: Comparison of corrosion potentials of Sn-rich alloys in 3.5 wt% NaCl solution 22

Table 4.1: Recorded time at circuit failure... 31

University of Malaya

List of Symbols and Abbreviations

Sn	: Tin
Ag	: Silver
Cu	: Copper
Zn	: Zinc
Bi	: Bismuth
Ni	: Nickel
Al	: Aluminium
In	: Indium
Pb	: Lead
e^-	: Electron
O_2	: Oxygen
H_2	: Hydrogen
SO_4^{2-}	: Sulphate

University of Malaya

1.0 INTRODUCTION

1.1 Study background

The main material of choice for solder within the early 1960s was predominantly tin-lead (Sn-Pb) due to the material's low melting temperature, good solderability and excellent corrosion resistance properties. However, EU's Restriction of Hazardous Substances (RoHS) effective July 2006 saw the prohibition of the use of heavy metals, including Pb, in electrical and electronic equipment in the European Union (George & Pecht, 2016). This was due to environmental and health concerns from the disapprobation toxicity of lead. The effect of this ruling was widely felt by the electronics industry due to the previous widespread use of lead, and much research was made to present several potential substitutes to fulfil the demands of the void left behind by Sn-Pb.

However, the explosive growth of surface mount (SMT) technology in light of the high demand for more powerful devices in a fraction of the footprint would present another obstacle. This drive towards miniaturisation saw a shift in demand to higher-density printed circuit boards with that would require a higher electrical gradient to power its components, subsequently causing an overall higher heat flow (Zhong, Chen, et al., 2017). Such was found to cause an increase in the risk of mechanical failure from various sources e.g. whiskering and fatigue at the solder joints (J.-X. Wang et al., 2009).

Electrochemical migration (ECM) is one of such issues that has become a forefront topic with this new growth within the microelectronics industry. Defined as a process where a metal placed under an electrical potential and in contact with insulating materials would undergo ionic transfer from one location to another location (Zhong, Chen, et al., 2017), this phenomenon would cause a variety of problems. An example of such include including corrosion and the reduction of surface resistance (L Hua & Yang, 2011).

University of Malaya

The combination of these conditions and issues led to the discovery of Sn-Ag-Cu as a promising candidate to replace Sn-Pb. It not only possessed comparable physical properties such as microstructure, but also decent wettability (Efzan Mhd Noor & Singh, 2014). However, a study conducted by Zhang et al. (2012) found that SAC solders were not necessarily suitable for universal application due to poorer wettability compared to Sn-Pb and high melting temperature. To this end, it was found to be necessary to dope the current existing bulk alloy with various elements (e.g. Zn, Bi, Al) to further improve the usability of these SAC solders.

One of such elements studied was zinc (Zn). Not only did it have the advantage of low cost, it also had a low reflow temperature and comparable mechanical properties to Sn-Pb, making it an ideal substitute for the material (El-Daly et al., 2009). Tsao et al. (2010) meanwhile found that the addition of Zn to SAC alloys could reduce the melting temperature of the alloy by 2°C, while another study by Kotadia et al. (2012) noted that the addition of Zn had improved the microstructure by suppressing the voids in the lattice. Another study by Lin and Chuang (2010) noted that the tensile strength of the alloy had also increased upon addition of Zn.

However, due to their higher position within the electrochemical series, alloys containing Zn are more susceptible to corrosion. This has become an area of concern with the aforementioned promising nature of Zn, prompting many studies to be conducted on the improvement of the performance of such alloys.

There exists however a gap in current research with regards to the effect of small incremental Zn addition on SAC305 alloys. Most current research only explore the effects of large dosages of Zn on SAC305 on the electrochemical migration process and/or focus on the effects on the corrosion process that occurs after the electrochemical migration process. The differences within the phenomenon (i.e. the lifetime and the failure process)

University of Malaya

thus still remain largely undocumented. This study seeks to address this lack of information.

1.2 Study objectives

The aim of this research project is to understand the effect of Zn addition as a fourth element on the electrochemical migration process of Sn-3.0Ag-0.5Cu solder alloys. This study will endeavour to fulfil the following objectives:

i. To investigate the effect of zinc addition on the time to failure of Sn-3.0Ag-0.5Cu solder alloys
ii. To investigate the effect of zinc addition on the topology of dendrites formed during the electrochemical migration process.

1.3 Scope of the study

This study's main focus is on the ECM process and the failure mode of Zn-doped Sn-3.0Ag-0.5Cu alloys under corrosive environment. This will be studied via an increase of Zn content within an SAC alloy subjected to a water-drop test. The Zn content will be varied but will not exceed 0.5% to allow for the observation of the effects of minute additions of Zn to the system. The ECM process tests will focus on the time to failure for the circuit setup, while the end result of the test will be analysed via surface electron microscopy (SEM) to understand the extent of damage caused by ECM.

University of Malaya

2.0 LITERATURE REVIEW

2.1 Introduction

Solder has been defined as a fusible metal alloy with a melting temperature of 90 to 450°C (Schwartz, 2014) that is used for the interconnecting and assembly process of electronic components, particularly on microcircuit boards. Tin (Sn) is one of the most common materials used in solders, with the eutectic Sn-Pb solders previously one of the most commonly found solders in the microelectronics industry. This was attributed to their low cost and melting temperature, as well as their good solderability and mechanical properties (Mohanty & Lin, 2006).

However, due to mounting concerns from environmental and health perspectives, several Sn variants have been proposed to replace Sn-Pb, such as Sn-Ag, Sn-Zn, Sn-Ag-Cu, Sn-Zn-In etc. The choice of maintaining Sn in the solder systems was due to their properties, microstructures and costs, that were considered to be the best amongst lead-free alloys (Hassam et al., 1998).

Despite this, the proposed binary and ternary Sn-rich systems are still unable to meet the needs of microelectric packaging, necessitating research into the inclusion of additional rare-earth alloying elements (e.g. Zn, Bi, In) into the structure for performance improvement. In addendum to having comparable performance to Sn-Pb solders, the substitute materials are also expected to have good corrosion resistance.

This is because corrosion resistance has become a criterion following the push to miniaturisation of electronic components, as the closer proximity of two different metallic components may result in corrosion (e.g. electrochemical migration, galvanic, pitting, etc). Furthermore, the exposure of microelectronics to different environments of varying humidity, pollutants and temperature also affects the rate of corrosion in the components (Andersson & Liu, 2008; Kotadia et al., 2012).

University of Malaya

A large concern about corrosion in solder alloys is due to the ability to affect the structure of the metallic alloy itself via introduction of crack initiation sites within corroded areas, in turn affecting the physical and electronic properties of the components joints themselves. This would ultimately lead to failure of components, and in today's microelectronics industries where each package comprises of hundreds of individual components, the failure of one component could very well spell the catastrophic failure of the rest of the circuit in the package.

To this end, it is necessary for any Sn-Pb solder substitute to ensure that they are comparable or indeed, superior to Sn-Pb solders themselves in their physical and performance characteristics. The push to further reduce the size of electronic products will continue, and such, the technology must continue to evolve to meet these needs.

2.2 Physical performance characteristics of lead-free Sn-based solders

As aforementioned in Section 2.1, a suitable Sn-Pb substitute must possess several characteristics to fulfil the requirements of today's microelectronics industries. These characteristics can be divided into two categories: Physical/mechanical properties and thermal/electrical properties.

In terms of physical and mechanical properties, a low melting temperature and good wettability is ideal for a solder to facilitate workability of the material without overconsumption of energy. Furthermore, as solder joints are subject to a high heat flux due to the magnitude of the electrical field gradient, they require good creep resistance. High tensile strength is also required for a longer lifetime of the joint.

In terms of thermal and electrical properties, solders are commonly used at joint areas to connect two components together. This necessitates a low electrical resistivity to minimise the heat generation and required voltage for the current to pass through.

University of Malaya

However, considering the higher heat generation, the solder material must also have higher thermal conductivity to allow for faster heat dissipation from the joint.

Aside from the characteristics mentioned above, an ideal solder also must have good wettability. Dušek et al. (2016) classifies wettability into two major factors: Wettability level and wettability speed. The wettability level will affect the contact angle and surface energy of the interface, while the wettability speed controls the ability of the liquid to spread across a surface (Nurul Liyana, 2018). A good solder should have both; to ensure a good bond between the base metal and the solder, the solder should properly wet the surface of the metal.

Whilst many Sn-rich alloy variants exist, this review will only look at the most studied variants. A comparison of the most common solder alloys can be found in Table 2.1 below:

Table 2.1: Comparison of performance characteristics of commonly used solder alloys

	Sn-Pb	**Sn-Ag**	**Sn-Ag-Cu (SAC)**	**Sn-Zn-Al**
Melting point (°C)	183	221	218	199
Tensile strength (MPa)	41	61	35	46
Yield stress	28	23	27	27
Thermal conductivity (W/[m.K])	50	55	55	66
Electrical resistivity (μΩ.cm)	15	12	11	34-58
Reference	(Yamamoto & Tsubone, 2007)	(Smith et al., 2002)	(Yamamoto & Tsubone, 2007)	(Yamamoto & Tsubone, 2007)

It can be observed that SAC has very similar properties to Sn-Pb, making it a viable substitute for Sn-Pb.

University of Malaya

2.2.1 Performance comparison between SAC105 and SAC305

There exists, however, several variants of SAC alloys as well. The two variants given focus in this review are 98.5% Sn-1% Ag-0.5% Cu (SAC105) and 96.5% Sn-3% Ag-0.5% Cu (SAC305), in which the difference between the two stem from the additional 2% silver in the alloy. The mechanical properties of SAC105 and SAC305 are detailed in Table 2.2 below.

Table 2.2: Comparison of performance characteristics of SAC105 and SAC305

	SAC105	**SAC305**
Solidus temperature	217	217
Liquidus temperature	226	222
Elastic modulus (GPa)	43	51
Yield strength (MPa)	29	30
Ultimate tensile strength (MPa)	25	38
Reference	(W. Liu & Lee, 2007; Sabri et al., 2013)	(W. Liu & Lee, 2007; Sabri et al., 2013)

Further studies by Che et al. (2008); Che et al. (2007) indicate that the increase in Ag content resulted in an increase in the ultimate tensile strength, yield strength and Young's modulus. This was attributed to the changes in the microstructure and the intermetallic compound (IMC) distribution. Sn grain size was also found to be finer with higher Ag content, resulting in fewer plastic deformations of the solder alloy.

Sabri et al. (2013) however argues that the higher Ag content of SAC305 would result in a lower drop impact reliability due to its lower bulk compliance and plastic energy dissipation. This observation was confirmed by a study conducted by W. Liu and Lee (2007) that found that SAC105 had a minimum drop rate of 5.1 compared to 1.2 of SAC305. However, Sabri also observed that the reduced Ag content also compromised the thermal mechanical fatigue properties of the alloy, an observation proved by Henshall et al. (2009) who observed hard-open cracking was observed for SAC105 at 3291 thermal cycles, compared to the superior 6657 cycles for SAC305. This indicated that the thermal fatigue life of SAC105 was inferior to that of SAC305.

University of Malaya

A balance thus must be struck between the impact resistance and the fatigue properties of the alloy which may prove to be difficult with the limitations of a ternary system. To this end, studies would propose the incorporation of other elements into the alloy structure to compensate for the weakness of these SAC alloys.

2.2.2 Influence of element addition on Sn-rich alloys

As outlined in Section 2.2, SAC alloys are comparable for most properties, primarily in joint strength. However, many problems have still been reported for SAC such as the formation of voids in interfacial IMCs, higher IMC growth rate, large undercooling during the solidification process, and the spalling of interfacial IMCs during high temperature storage (Cho et al., 2007). These problems become of particular importance during high temperature application as higher IMC growth results in a higher concentration of brittle IMCs (J. Li et al., 2007). This increase in brittleness lead to the formation of voids and coalescence in the Cu_3Sn IMCs, resulting in crack formation at the solder joint interface (Kotadia et al., 2012). As automotive and aerospace may subject these alloys to high temperatures of up to 150°C, this becomes a cause of technological concern (Kotadia et al., 2012).

Studies have thus turned to the incorporation of other elements, i.e. Zn, Bi, Al, Ni, In, etc into the alloy to suppress the formation of voids within the alloy. A summary of the properties imparted by these elements compared to that of Sn can be found in Table 2.3.

University of Malaya

Table 2.3: Comparison of performance characteristics for additional alloying element in Sn-alloys

Element	Melting point	Wettability	References
Tin (Sn)	-	Good	(Xu et al., 2006)
Zinc (Zn)	Lowers	Improves	(El-Daly et al., 2009; Kanlayasiri & Meesathien, 2018)
Bismuth (Bi)	Lowers	Improves	(Choi et al., 2002; Y. Liu et al., 2014)
Nickel (Ni)	Increases	Improves	(El-Daly et al., 2013; Y. Wang et al., 2009)
Indium (In)	Lowers	Lowers	(Puttlitz & Stalter, 2004)

Zn is one of the most common alloying elements for SAC because of its low cost and low reflow temperatures that allow it to substitute Sn-Pb solder without increasing the soldering temperature (El-Daly et al., 2009). A small Zn dosage in an alloy was found to refine the microstructure of the bulk alloy while suppressing IMC growth during thermal aging which would otherwise have resulted in a brittle solder joint (Wang et al., 2005). However, Zn is a more reactive material compared to Sn as it's higher on the electromotive force series; as thus, it will be subject to corrosion much faster than Sn. This will be further discussed within Section 2.3.4.

Bismuth, meanwhile, has been reported to impart superior soldering properties e.g. high joining strength, comparable melting temperature and good wettability (El-Daly et al., 2009). El-Daly's study also observed that the tensile strength, ductility and the tendency for necking was further improved upon by addition of Bi.

The addition of Ni was found to decrease the thickness of the IMC layer between the substrate and the solder when added to SAC in small amounts (Yakymovych et al., 2018).

University of Malaya

However, there was no significant difference noted in the microstructure and mechanical properties of the solder joints upon addition of Ni.

The use of In in SAC305 was reported to increase the ultimate tensile strength and hardness of the alloy due to the secondary phase dispersion and the strengthening effect of the solid solution (Sungkhaphaitoon & Chantaramanee, 2018). The eutectic liquidus temperature was also found to have improved; however, the ductility of the alloy was found to have decreased for all alloys containing In.

From these options, Zn and Bi present the most promising potential to address the shortcomings faced by SAC305. Due to this, several studies have been done on the effect of Bi addition to SAC alloys in both low (Mahdavifard et al., 2015) and high dosages (El-Daly et al., 2009). Conversely, Zn-centred studies in the perspective of SAC alloy improvement primarily deal with high-Zn content SAC alloys to take advantage of Zn's excellent mechanical properties (Li Hua et al., 2011; J.-C. Liu et al., 2015; Tanaka, 2002), though studies on low-Zn content SAC alloys remain very far and in between. There remains an opportunity thus to study the improvement capabilities of SAC solders via addition of Zn, but care must be taken about the chemical properties of Zn before choosing it as a replacement for Sn-Pb.

2.3 Chemical properties of solder alloys

As a metal, SAC alloys face a wide range of typical chemical-based corrosion processes that may hamper its long-term durability and performance. Examples of such are galvanic corrosion, whiskering, electrochemical migration, etc.

The focus of this paper will be on electrochemical migration (ECM).

2.3.1 The electrochemical migration (ECM) process

Defined as the transport of metal ions between two oppositely biased electrodes via a continuous electrolyte (Medgyes et al., 2015), ECM is an increasingly common form of

University of Malaya

corrosion faced by the microelectronics industry due to the push towards higher density PCBs. As sizes of circuits shrink, the thickness of the (continuous) invisible adsorbed vapour layer e.g. water vapour from the humidity in the surroundings on the surface of the components will rise, making components and solders alike more susceptible to corrosion. This will lead ultimately to failure of the components.

ECM commonly involves three major reaction processes: The anodic dissolution of metal, the transport of metal ions and the electrodeposition of ions (Lloyd et al., 2006). In detail, when a voltage difference is applied between two electrodes, parts of the metal at the anode will be ionised and will migrate towards the cathode to be deposited (Zhong, Chen, et al., 2017).

These processes can be observed visually via the formation of microscopic metallic dendrites that bridge the anode and the cathode during the length of the ECM phenomenon; an example of it has been pictured in **Figure 2.1**. When a dendrite bridges the two electrodes together, it results in insulation-resistance degradation or short-circuit failure of the components (Jiang et al., 2018). Care must be taken however to distinguish between ECM and the whiskering process; the latter is a solid-state corrosion process and even though both involve dendrite formation, only ECM involves the dissolution of metal and the presence of an electromagnetic field (Sarveswaran et al., 2017).

There are many factors that may affect the rate of ECM: The presence of contaminants within the electrolyte layer, the magnitude of applied voltage, the distance between the two electrodes, and even the composition of the electrolyte layer itself may play a role in the acceleration of ECM within a system. To observe and compare the effects of each of these factors, there exists a few commonly used test methods to characterise the ECM corrosion process.

University of Malaya

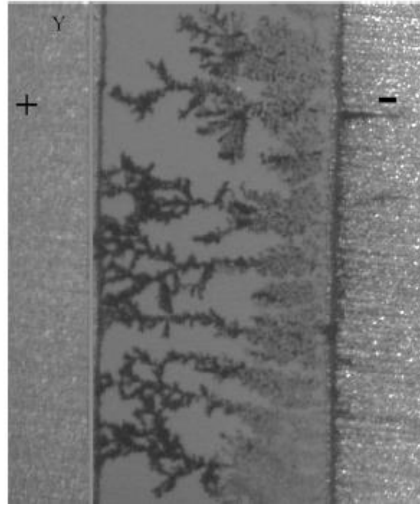

Figure 2.1: Dendrite formation bridging the gap between the anode and cathode (He et al., 2014)

2.3.2 Electrochemical migration tests

Three common tests are primarily used to evaluate the progress and extent of ECM in a system: The water drop test (WD), thermal humidity bias test (THB) and thin electrolyte layer test (TEL). A comparison of the three methods have been drawn below in Table 2.4.

.

University of Malaya

Table 2.4: Comparison of ECM corrosion test methods

	WD	THB	TEL
Controllable factors	- Rate of transfer - Electrolyte layer thickness - Contaminant concentration	- Temperature - Relative humidity	- Electrolyte layer thickness - Contaminant concentration
Length of test	Several seconds to a few minutes	Lifetime of component/circuit	Several seconds to a few minutes
Advantages	- In-situ monitoring - Fast - Contaminant concentration known	Can simulate actual operating conditions	- Known electrolyte layer thickness - In-situ monitoring
Disadvantages	- Electrolyte layer formation process cannot be simulated - Distance between electrode and electrolyte drop cannot be controlled	- Unknown electrolyte thickness - Difficult for in-situ monitoring	- Electrolyte layer formation process cannot be simulated - Cannot be used to simulate practical application

Ref: (Zhong, Guo, et al., 2013; Zhong, Yu, et al., 2017)

University of Malaya

The WD test is commonly used for laboratory studies and involves placing a drop of electrolyte of known volume onto the surface of the sample between the electrodes under a bias voltage as pictured in **Figure 2.2(b).** The setup is connected to a picoammeter to monitor the fluctuations in the current in the system as pictured in **Figure 2.2(a).** When a short circuit happens, a significant spike will be observed in the current, denoting failure of the material. The test primarily measures a material's time to failure via ECM as the test duration is no longer than a few minutes (Dominkovics & Harsanyi, 2008).

The major advantage of this test is the ability to control the composition and concentration of the electrolyte layer i.e. by controlling the contaminant content. However, this test can only be used to simulate tests with visible electrolyte layers due to the thickness of the electrolyte layer, making it unsuitable to model practical in-line

situations that may require adsorbed invisible electrolyte layers. The WD test is unable, thus, to model the electrolyte formation process.

There is also no standard as to the amount of electrolyte that should be used for WD tests, with the volume of the water droplet reported to be between 10 to 20 μL in some publications (Dominkovics & Harsanyi, 2008) and up to 3mL in some others (Yu et al., 2006). The location where the electrolyte drop is placed as well is not fixed, leading to an inconsistent contact area between the electrode and the electrolyte drop.

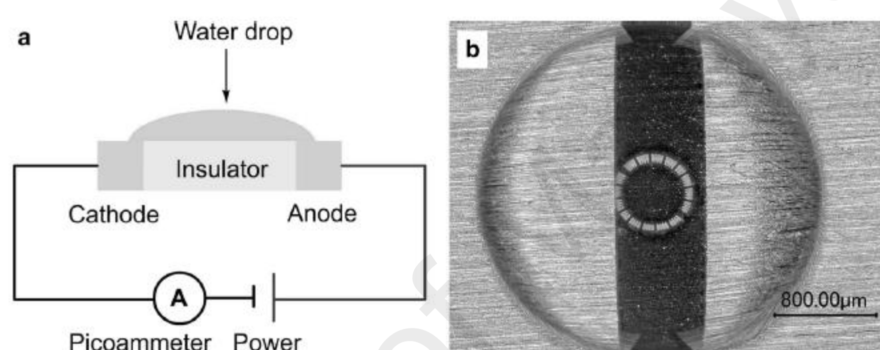

Figure 2.2: (a) Water drop test setup; (b) Optical graph of test setup at the beginning of a WD test experiment (Zhong, Yu, et al., 2017)

The TEL test, as pictured in **Figure 2.3,** meanwhile, is similar to the WD test with several differences. A thin electrolyte layer is placed on the sample surface under an applied bias voltage. A needle connected to a micrometer measures the thickness of the electrolyte layer, while the potentiostat measures the current within the circuit. The major difference between this method and the WD is the shape of the electrolyte; the WD employs spherical electrolyte, while the TEL uses a horizontal thin layer (Zhong, Yu, et al., 2017). This allows for higher reproducibility of the data.

However, similar to the WD test, the TEL test cannot be used to simulate the electrolyte layer formation process as the TEL itself has to be artificially made before the start of the test. The test is also heavily limited by the thickness of the TEL; a TEL of 30

University of Malaya

microns has been reported in studies (Zhong et al., 2015), but practical on-site thickness of electrolyte layers may realistically be lesser than that.

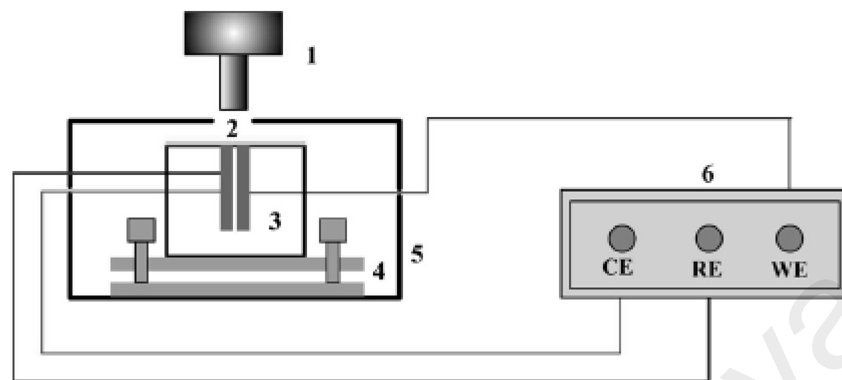

Figure 2.3: Schematic for thin electrolyte layer test: (1) 3D microscope, (2) thin electrolyte layer, (3) electrode, (4) horizontal stage, (5) glass chamber, (6) potentiostat (Zhong, Guo, et al., 2013)

Conversely, the THB test is capable of addressing these very drawbacks from both tests. The THB test is usually conducted within a humidity chamber that allows for manipulation of temperature and relative humidity in the environment. This allows for the invisible (i.e. adsorbed) electrolyte layer to form on the surface of the component, making this method the closest to the actual operating environment of an electronics system. To ensure consistency of THB methodology as well, several standards are currently in existence e.g.IPC J-STD-004B, Bellcore, JIS Z 3197 (Puechagut et al., 2015). In the case that accelerated testing may be require, it is also possible to run more severe THB tests, with temperatures up to 85°C and relative humidity up to 99% (Zhong, Yu, et al., 2017).

However, there are certain disadvantages to running the THB test as well. Due to the nature of the invisible electrolyte layer, it is difficult to ascertain the composition of contaminants present within the electrolyte, as well as the exact thickness of the electrolyte layer itself. As a higher layer thickness would no doubt affect the rate of the

University of Malaya

ECM reactions (Nishikata et al., 1997), this would require a larger pool of data to ensure consistent results. The THB test also faces hardware complications for in-situ monitoring, as it may be difficult to find a camera lens capable of functioning under high relative humidity and temperature. The finer details of the ECM process such as the structure of the dendrites unfortunately is not clear from any graphical data that can be obtained as well (Zhong, Yu, et al., 2017).

2.3.3 ECM corrosion mechanisms of SAC alloys

As previously mentioned in Section 2.3.1, ECM primarily consists of three processes: Anodic dissolution, ionic transfer and cathodic electrodeposition. There is however one step that prefaces this: The electrolyte layer formation.

ELECTROLYTE LAYER FORMATION

This step is necessary to create a path between the cathode and anode; without an electrolyte layer, ECM cannot occur. A study by Lee and Staehle (1997) found that the sufficient number of electrolyte layers to start the corrosion process on a metal surface is at approximately 60% to 70% at room temperature, depending on the substrate surface energy and polarity. This number, however, is subject to change based on the contaminants contained within the electrolyte, as the presence of different contaminants affect not only the ECM time (Jung, Lee, Joo, et al., 2008), but also the critical humidity. Rice et al. (1982), for instance found that this figure can go as low as 40% while maintaining a thickness equivalent to several monolayers.

From a corrosion perspective, the thickness of the layer affects the ECM process, with studies showing that dendrite growth and morphology could be affected by the electrolyte layer thickness. A study by Warren et al. (1989) found that dendrite growth rates and morphology were similar for TEL and bulk solution (i.e. WD test) situations, but significantly different in the case of adsorbed moisture layers. This was proven by a study

University of Malaya

by Jiang et al. (2018) who found that the mean time to short circuit for SAC305 would gradually increase as electrolyte layer thickness was increased till it peaked at an optimum thickness and decrease upon further addition of electrolyte layer thickness. This indicates that the electrolyte layer thickness may indeed hinder or facilitate the ECM process depending on the sufficiency of the layer thickness. Likewise, a study by Zhong et al. (2015) found that the dendrite growth rate could increase until an optimum level before it starts to decrease again, based on the thickness of the electrolyte layer.

However, as mentioned in Section 2.3.2, this step is only significant in the case of THB tests, as WD and TEL tests cannot simulate it.

ANODIC DISSOLUTION

Takemoto et al. (1997) first theorised that that the large rate of dissolution at the anode was responsible for a high ECM susceptibility in solder alloys. However, SAC305 contains three different potential metals present at the anode capable of oxidation, indicating that one must be the rate-determining step.

To this end, Jung, Lee, Lee, et al. (2008) found that the dissolution of Sn was the rate-determining step in an SAC305 system, and that microelements (e.g. Ag, Cu) do not participate in the ECM as they will have formed chemically stable intermetallic compounds with Sn. This finding was confirmed by Yi et al. (2019) and Li Hua et al. (2011) who found that 95% of SAC305 dendrites were Sn. The dissolution reaction would thus follow these reactions:

$$\mathrm{Sn} \rightarrow \mathrm{Sn}^{2+} + 2\mathrm{e}^{-} \qquad (1)$$

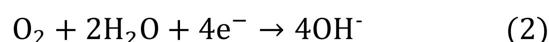

$$\mathrm{O_2} + 2\mathrm{H_2O} + 4\mathrm{e}^{-} \rightarrow 4\mathrm{OH}^{-} \qquad (2)$$

University of Malaya

Reaction (1) represents the oxidation of tin at the anode, while reaction (2) represents the reduction reaction at the cathode for oxygen within the moisture in the electrolyte layer.

Assuming reaction (1) as the rate determining step, several factors influence the rate of this step. Jiang et al. (2018) found that increasing the bias voltage applied by 2V to SAC305 could decrease the mean time to failure by at least 70%.

However, reaction (2) may not necessarily be the only reaction occurring within the system unless the entire system is fully sterilised and only contains distilled water. For systems with contaminated electrolyte layers (as in most actual practical cases), species of contaminants may affect the rate of ECM. A study by Jung, Lee, Joo, et al. (2008) found, for instance, that the ECM lifetime of pure Sn systems containing Cl^- ions was longer than that containing SO_4^{2-} ions by 27 seconds with a higher pitting potential.

Furthermore, the concentration of the contaminants play a role in the ECM rate as well. Yi et al. (2019), for instance, found an increasing trend in the time to short circuit upon increasing Cl^- ion concentration. This was inferred to be due to the presence of more hydroxide ions within the system, as well as a stronger disturbance from the evolution of hydrogen.

These various factors demonstrate that the anodic dissolution reactions play a significant role in influencing the ECM mechanisms not only at the anode, but also as an overall.

IONIC TRANSFER

Ionic transfer in an ECM system occurs in two directions: The positively charged metal ions at the anode will move towards the cathode, while the negatively charge hydroxyl ions at the cathode will move towards the anode. This transportation process occurs under

University of Malaya

an electric field and may occur via three different methods: Electrical migration, diffusion and/or convection.

Transportation via electrical migration is primarily determined by the migration velocity of the ion and can be expressed as per Equation 3:

$$v = \mu E \qquad (3)$$

where v is expressed as the ion velocity m/s, while μ and E express the ion mobility and magnitude of the electric field in terms of $m^2V^{-1}s^{-1}$ and Vm^{-1} respectively. Within ECM cases, μ is defined as a function of the ion characteristics (charge, shape, size) and the physical properties of the electrolyte (viscosity, pH, etc). Meanwhile, E is a function of the distance between the electrodes and the applied bias voltage (Bockris & Reddy, 1970).

Transport via diffusion, conversely, functions on a concentration basis. The higher concentration of cations at the anode and the lower concentration at the cathode provides a driving force for the ions to move from the anode to the cathode to achieve equilibrium. A study by Fukami et al. (2007) reported that dendrite formation was diffusion-limited based on the surface instability at the applied voltages. These diffusion-limited systems could be expressed by Laplacian fields, with the aforementioned instability caused by the far-equilibrium conditions at the electrodes (L Hua & Yang, 2011).

The last transport method, convection, is a method that is more applicable for corrosion systems in condensed conditions i.e. with an adsorbed invisible electrolyte layer (e.g. in THB test studies) compared to those in bulk-transport systems. This is attributed to the movement of the bulk electrolyte; in cases where electrolyte movement is minimal and of high thickness, it is assumed to be stagnant with negligible natural convection effects (Simillion et al., 2016). To illustrate, a source of strong convection was proposed to be the collapse of hydrogen bubbles at the cathode as the product of H^+ reduction (Noh et

University of Malaya

al., 2009). In the case of a large electrolyte layer, the instability caused by this reduction process would be considered insignificant to the overall transport equation in comparison to the other two transport mechanisms.

CATHODIC DEPOSITION

Upon reaching the cathode, the Sn ions will undergo a deposition process and be converted into Sn atoms as described in reaction (4).

$$2Sn^{+} + 2e^{-} \rightarrow 2Sn \qquad (4)$$

The final shape and morphology of the electrodeposit highly rely on the path of current flow and the concentrations of species involved (Sun et al., 2013). Areas with high solution resistance and difficulties in transport may become ion-rich, becoming preferential nucleation and growth areas for dendrites at the cathode.

The dendrite formation process consists of two stages: initiation and propagation. Two prerequisites are required for dendrites to form in a system, however: A precursor and a critical overpotential. Zhong, Chen, et al. (2017) states that the overpotential is usually represented by a critical bias voltage applied across the anode and cathode. Below this critical voltage, ECM and by extension, the dendrite formation process would not occur. Takemoto et al. (1997) observes this very phenomenon upon studying ECM in Sn-Pb alloys, noting that ECM did not occur below a holding voltage of 0.7V. Shyu (1983) in their study further observed that critical overpotential could be expressed as a function of exchange current density and the growth rate.

The dendritic precursor, meanwhile, is needed to initiate the process and determine where the preferential nucleation will start (Zhong, Chen, et al., 2017).The precursor disturbs the flow of current towards the cathode, causing the deposition rate on the precursor to be higher than the areas around it. This generates a protrusion which gradually develops into a dendrite.

University of Malaya

The propagation reaction occurs at a higher rate than the initiation stem as proven by various studies (He et al., 2014; Zhong, Zhang, et al., 2013) and is commonly fastest at the tips of a needle or tree-like shaped dendrites. Dendrites for SAC alloys are commonly more fern-shaped, as can be observed in **Figure 2.4**. The higher rate was attributed to two reasons: The first of which is the shorter distance between the dendrite tip to the anode compared to the rest of the electrode. This causes a stronger electrical field to be formed at the tip, which would further disrupt the current flow thus causing further deposition to occur (Minzari et al., 2011).

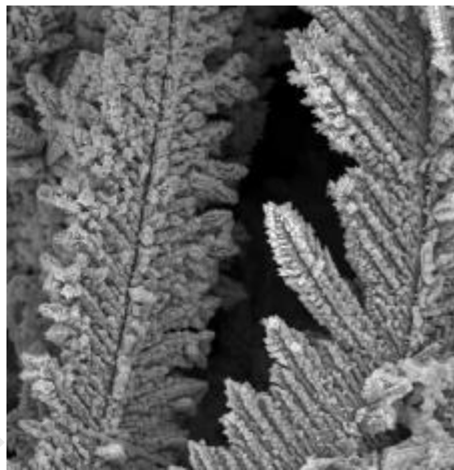

Figure 2.4: SEM image of SAC305 alloy dendrites after 70h ECM test in 3.5 wt% NaCl solution(L Hua & Yang, 2011)

Steppan et al. (1987) proposes an alternative reason: The formation of a sharp dendrite changes the diffusion process from a previously linear diffusion system to a more spherical diffusion of metal ions, increasing the rate of deposition of ions at the tip compared to the rate of deposition on the entire electrode.

Once the dendrite from the cathode reaches the anode, a short-circuit will occur, leading to the failure of the system. These dendrites can be observed via surface characterisation techniques, such as scanning electron microscopy (SEM).

University of Malaya

2.3.4 *Influence of element addition on the ECM performance of Sn-rich alloys*

Just as in the case of mechanical properties, the addition of different metals into the SAC alloy microstructure also affects the ECM and corrosion performance of the alloys themselves. This encompasses not only the rate of corrosion, but also the morphology of the formed dendrites. The former occurs due to the position of the added element into the alloy. Should the added element be higher on the electromotive force series than Sn, this causes it to function as a sacrificial anode, thus accelerating the corrosion process.

An example of this is the addition of zinc to SAC alloys. According to the *emf* series, Zn^{2+} is higher in the chart compared to Sn^{2+} and H^{+}. making it more electrochemically active than the other two species. Zn would thus be favoured more for electrochemical migration, leading to a higher rate of corrosion. Yu et al. (2006) investigated this in depth and found that Zn would always migrate compared to Sn, which indicated that alloys containing Zn would always have a higher susceptibility to ECM. Both L Hua et al. (2010) and Nazeri and Mohamad (2014) meanwhile studied the effect of adding Zn to Sn-Zn alloys and found that the additional Zn enhances the corrosion current density and subsequently, the corrosion rate.

Table 2.5: Comparison of corrosion potentials of Sn-rich alloys in 3.5 wt% NaCl solution

Element	Example alloy	Corrosion lifetime	I_{corr}	Reference
Pb	Sn-37Pb	-	8.14×10^{-3}	(Wu et al., 2006)
Ag-Cu	Sn-3.5Ag-0.5Cu	Longer	5.37×10^{-7}	(D. Li et al., 2008)
Zn	Sn-9Zn	Shorter	2.691×10^{-5}	(Wu et al., 2006)
Bi	Sn-8Zn-3Bi	Longer	1.38×10^{-5}	(Chang et al., 2004)
In	Sn-3.5Ag-0.5Cu-9In	Longer	7.413×10^{-6}	(Wu et al., 2006)

where I_{corr} is defined as the corrosion current density.

University of Malaya

From Table 2.5, the large difference between the corrosion current density of Sn-37Pb and Sn-9Zn confirms what L Hua et al. (2010) and Nazeri and Mohamad (2014) had claimed regarding the reduction in corrosion resistance with the addition of Zn. This was further confirmed by a comparison between the studies conducted by Fayeka et al. (2017) and Jiang et al. (2018). Jiang found that the mean circuit failure time for SAC305 was higher than that of SA, while Fayeka et al confirmed that the I_{corr} of SAC305 was at least ten times the I_{corr} of SA.

Another effect of the addition of elements into alloys is the change in the dendrite microstructure. Dendrites from alloys doped with different elements will display different fractal dimensions which result in the dendrite itself adopting a different shape. The addition of Zn into an SAC305 alloy, for instance, changes the original SAC dendrite microstructure to a more "rose"-like one (pictured in as found by L Hua et al. (2010).

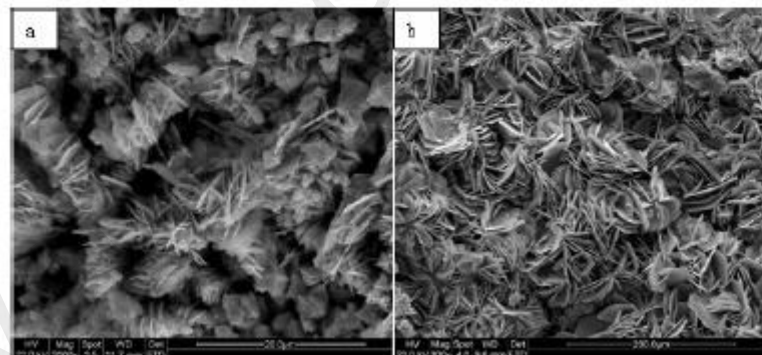

Figure 2.5: SEM of dendrite morphologies of SAC305 in 3.5 wt% NaCl (a, without metal doping; b, with added Zn) (L Hua et al., 2010)

With these facts in mind, Zn becomes a less attractive option on SAC alloys due to its susceptibility to corrosion. However, just as in the case of its mechanical properties, most papers that deal with Zn-containing SEM solders from an ECM perspective only approach the addition of this element in large doses, commonly of 1% and above (Li Hua et al., 2011; J.-C. Liu et al., 2015). It is still unknown if addition of minute amounts of Zn will

University of Malaya

yield the same results as those that added in bulk, and if the higher corrosion rate will also translate to an overall higher ECM rate as well.

2.4 Summary and conclusion

From the study of literature, several conclusions could be made:

1. To ensure that an alloy is a viable substitute for Sn-Pb alloys, it must contain at least comparable performance characteristics to Sn-Pb. This is especially important for the mechanical and electrical properties of the alloys.
2. Three types of tests are commonly used to evaluate the ECM process for a solder alloy: THB, WD and TEL. All three tests fulfil different needs and can be used concurrently to provide a holistic view of the ECM process.
3. The addition of foreign alloying elements (e.g. Zn, Bi, Ni) are capable of modifying these characteristics of the solder alloys. The result is a change in not only the rate of corrosion, but also the morphology of the end corrosion products.
4. SAC305 doped with minute additions of Zn presents an opportunity for study as too few research studies deal with the effects of minor Zn incorporation into SAC alloys compared to bulk alloying.

University of Malaya

3.0 RESEARCH METHODOLOGY

3.1 Introduction

This chapter describes the steps involved in the sample preparation, corrosion test and surface characterisation tests. There are three major stages involved in the conducting of this experiment: (a) The preparation of the mounted sample and the electrolyte solution; (b) Corrosion test via water drop (WD) test; and (c) Sample surface characterisation via scanning electron microscopy (SEM). The materials and apparatus used in this project are as listed below:

1) Lead-free solder alloys:
    a. Sn-3.0Ag-0.5Cu
    b. 99.9 [Sn-3.0Ag-0.5Cu]-0.1Zn
    c. 99.7 [Sn-3.0Ag-0.5Cu]-0.3Zn
    d. 99.5 [Sn-3.0Ag-0.5Cu]-0.5Zn
2) Polytetrafluoroethylene (PTFE) sheet
3) Sn24-Bi58 solder
4) Epoxy resin and hardener
5) Isopropyl alcohol
6) Sodium chloride (NaCl) powder
7) Electrical-discharge machine (EDM)
8) Polishing machine and silicon carbide (SiC) sandpaper
9) Water-drop test machine (Keithley)
10) SEM machine

University of Malaya

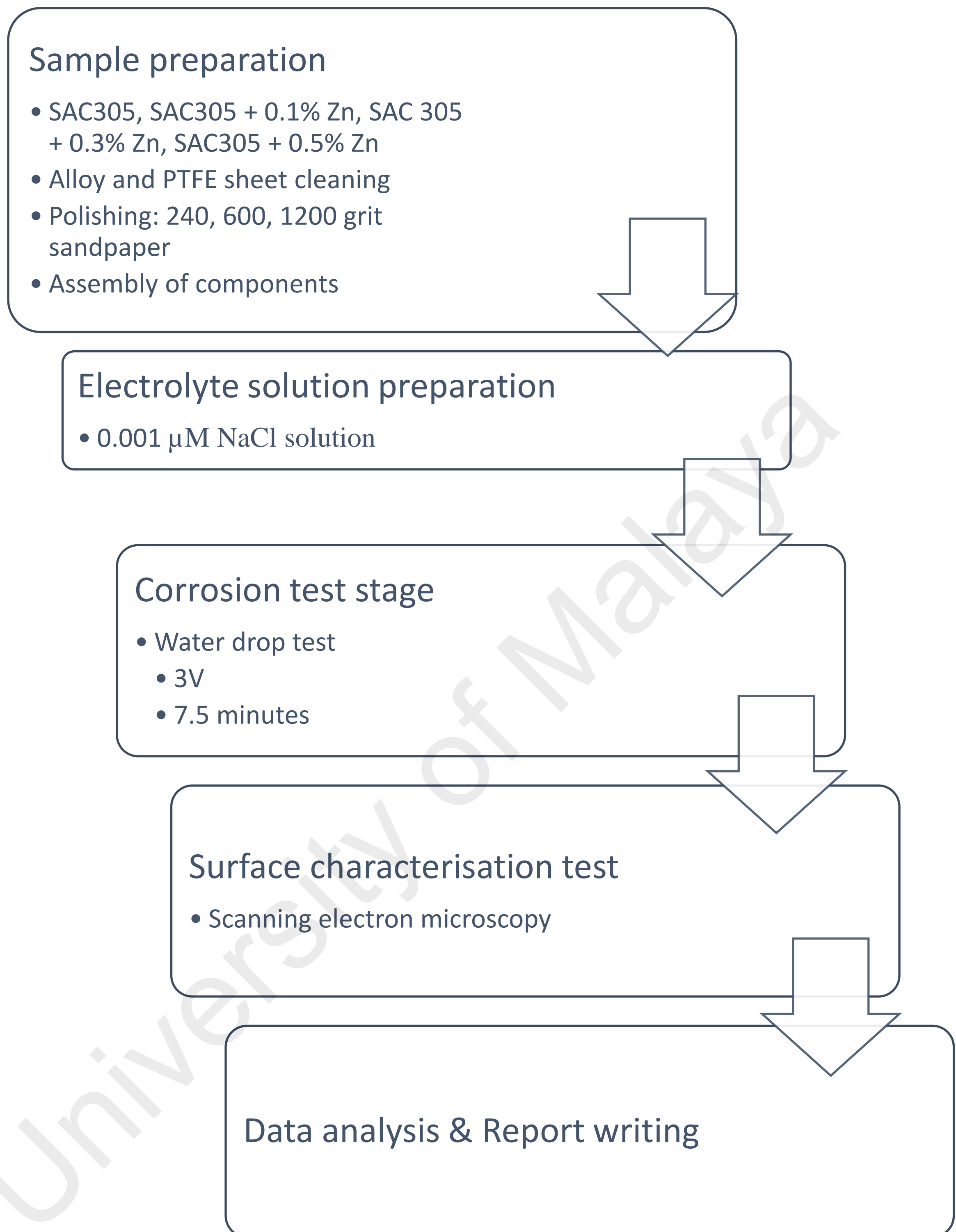

Figure 3.1: Flowchart of experimental procedure

The water-drop test and SEM surface characterisation test were chosen as they were the most common tests used in other similar studies. By choosing these two tests, easier comparison of results can be drawn for this study.

3.2 Sample and solution preparation

3.2.1 Sample preparation

Solders Sn-3.0Ag-0.5Cu, Sn-3.0Ag-0.5Cu-1.0Zn, Sn-3.0Ag-0.5Cu-3.0Zn and Sn-3.0Ag-0.5Cu-5.0Zn were wire cut via EDM into samples of 0.5mm thickness and1.5 cm width by 1 cm height. The back and front wider planes were polished with 150 grit silicon carbide paper to remove oxidation and mill scale from the surface. The alloys were then rinsed in isopropyl alcohol and distilled water to remove impurities before being force dried.

Simultaneously, 1.5 cm wide x 1 cm height coupons of PTFE were cut from a sheet of 0.5 mm thickness. These rectangles were first washed with soap solution before being rinsed with isopropyl alcohol and distilled water to remove impurities and subsequently force dried.

A length of copper wire was bent into an L-shape and attached to each solder alloy sample with Sn24-Bi58 solder.

All three components were assembled together as pictured in Figure 3.2 with plastic specimen clips. This assembly was mounted in cold moulds using epoxy resin.

After the demoulding process, the top of the mounted sample was polished with 240, 600 and 1200 grit SiC paper until the top surface was exposed.

University of Malaya

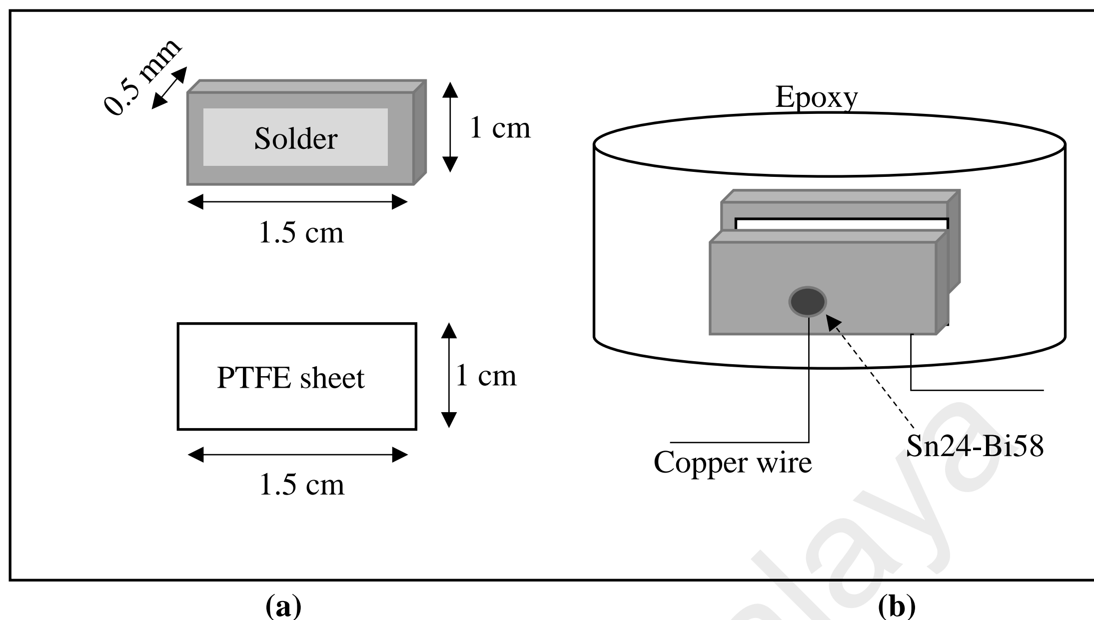

Figure 3.2: (a) Sample dimensions; (b) Full assembled system

3.2.2 Electrolyte solution preparation

The water drop test would use a solution of 0.001M. To obtain this solution, 0.00584g of NaCl was weighed and added to 100 ml of distilled water in a beaker. The solution was then stirred with a magnetic stirrer for 10 minutes to ensure complete homogeneity of the solution.

3.3 Electrochemical migration test

3.3.1 Water drop test

The sample was mounted on the jig of the test apparatus and the copper wires on the sample were connected to the anode and cathode respectively. 20 µl of electrolyte solution was pipetted onto the surface of the sample, with care taken for the electrolyte droplet to cover both electrodes. The machine then applied a stable 3V bias voltage across the sample and the reactions occurring on the surface of the sample were observed for 7.5 minutes. The electrical current running through the sample was also recorded as a function of time as well to collate with the visual observation during the water drop test.

University of Malaya

All tests were conducted at room conditions to maintain consistency.

3.4 Surface characterisation test

3.4.1 Scanning Electron Microscopy (SEM)

After the water drop test was completed, the sample surface was analysed by SEM at a 3V setting.

University of Malaya

4.0 RESULTS

4.1 Water drop test

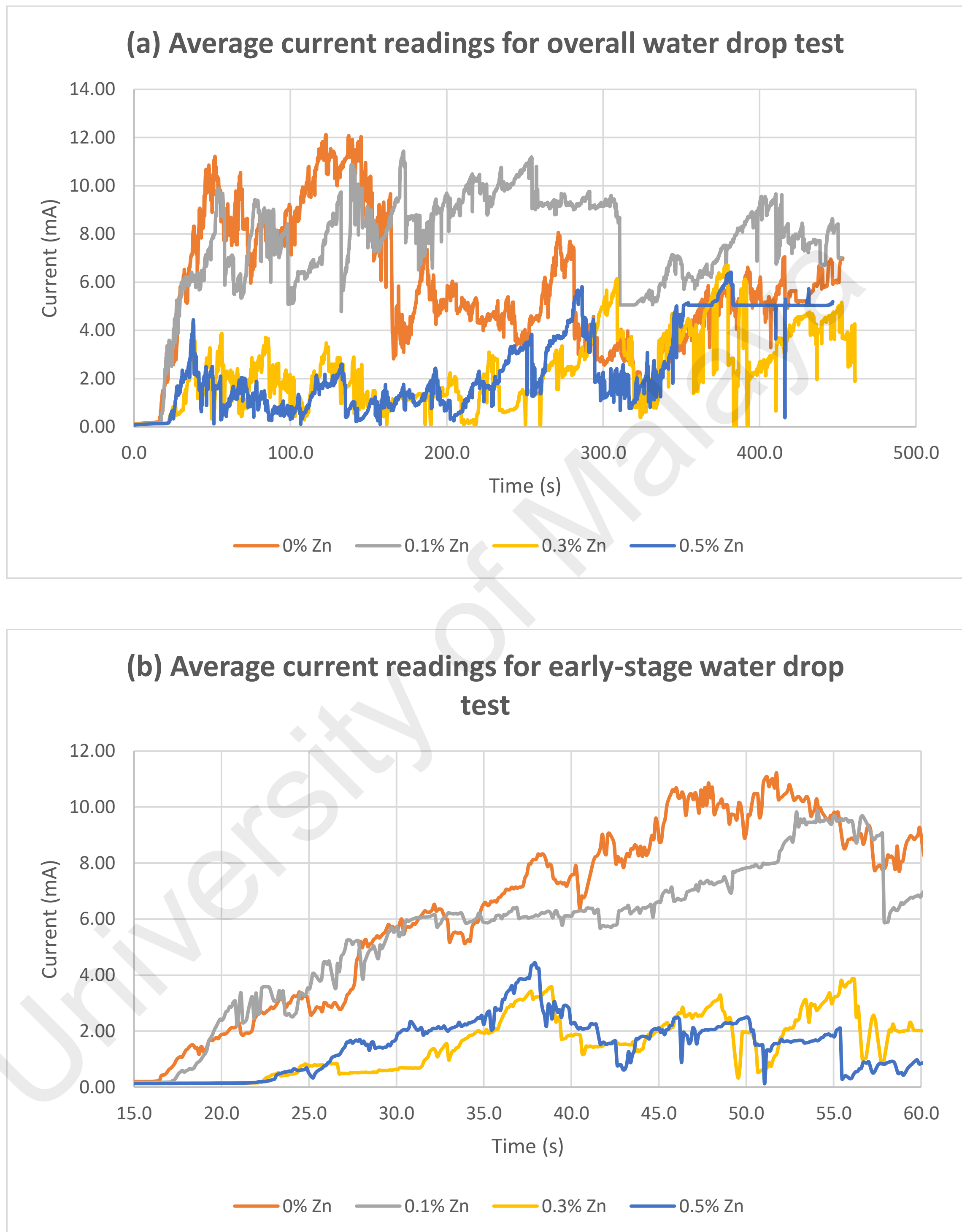

University of Malaya

Figure 4.1: Average current readings for Zn and non-Zn containing samples for water drop test

Figure 4.1 showed the average current readings recorded in the first 60 seconds of the water drop test for the four samples containing incremental content of Zn, as well as the overall current readings for the entire duration of the study. The time-to-failure (TTF) for each sample was recorded in Table 4.1.

Table 4.1: Recorded time at circuit failure

Zn content (%)	**Time-to-failure (s)**
0.0	18.285
0.1	20.787
0.3	23.271
0.5	24.870

4.2 Scanning Electron Microscopy

4.2.1 400x magnification

Increasingly heavy precipitation was observed when the Zn content of the solder alloys were increased, with the 0% Zn samples showing about 60% coverage of the PTFE sheet covered with precipitate and the 0.5% Zn sample showing approximately 90% coverage with precipitate.

University of Malaya

Heavy dendrite formation was observed primarily at both cathodes and anodes, but the larger clusters were observed to be situated primarily at the anodic area.

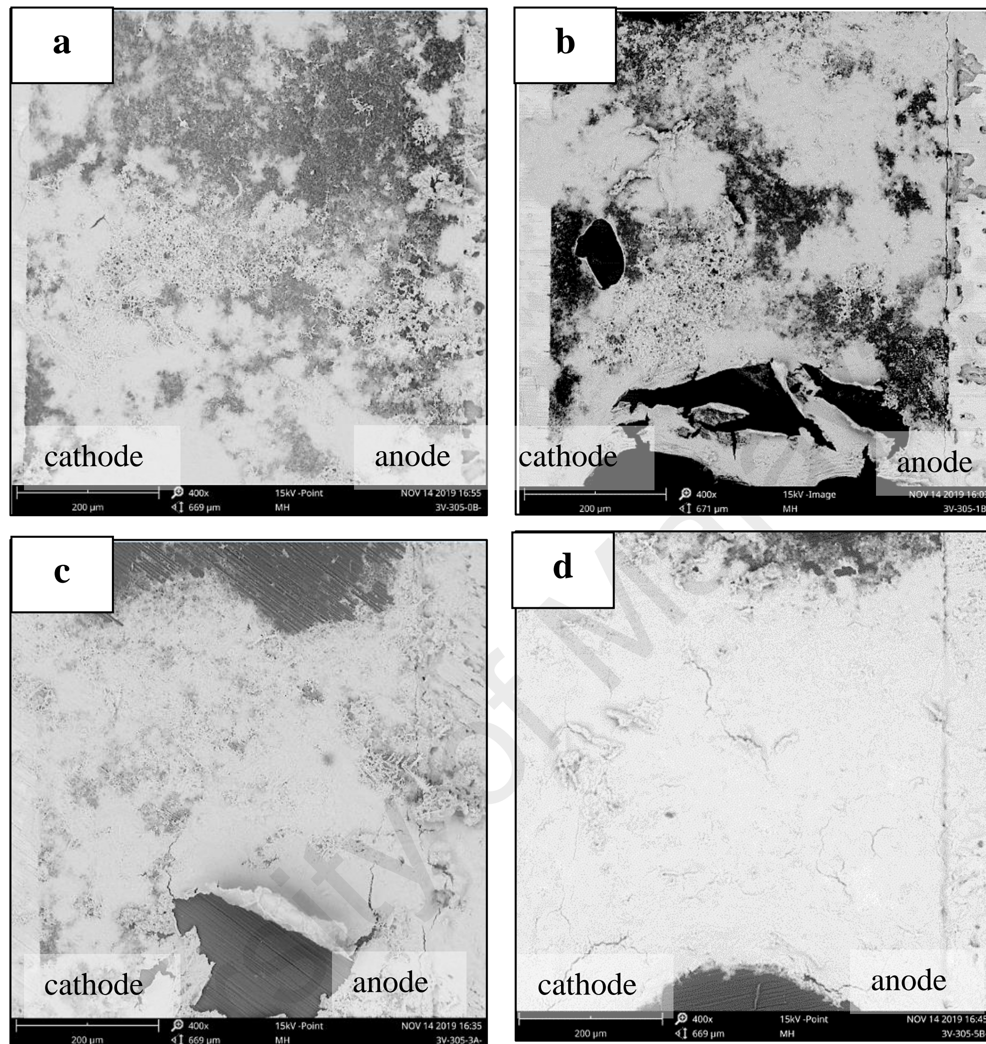

Figure 4.2: SE micrographs for SAC305 samples at 3000x magnification containing: (a) 0% Zn; (b) 0.1% Zn; (c) 0.3% Zn; (d) 0.5% Zn

4.2.2 10,000x magnification

Dendrite morphology for the 0% Zn sample was fern-shaped with large diamond-shaped bulbous protrusions observed at the tips. Dendrite clusters were thick with large spines in bulk growth.

Conversely, dendrite morphology for the 0.1% Zn sample was sharp and needle-like at the tips with a slightly thinner backbone. Dendrite clusters were thick but thinner than that of the 0% Zn sample.

Dendrite morphology for the 0.5% Zn sample however was observed to be fine and thin with a straw-like structure. The backbone of the sample was considered to be the thinnest amongst the samples.

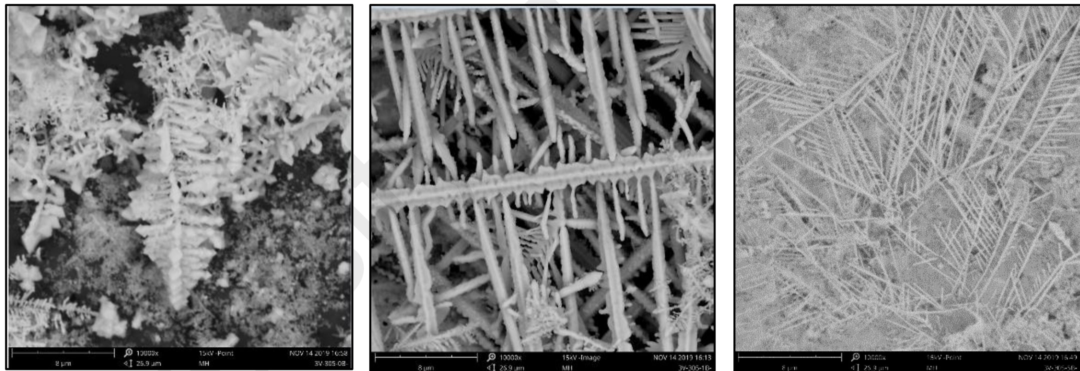

Figure 4.3: SEM micrograph at 10,000x magnification of SAC305 alloy dendrites with addition of: (a) 0% Zn; (b) 0.1% Zn; (c) 0.5% Zn

University of Malaya

5.0 DISCUSSION

5.1 Water drop test

5.1.1 Time-to-failure

Figure 5.0.1 shows the time to failure (TTF) for the water drop test.

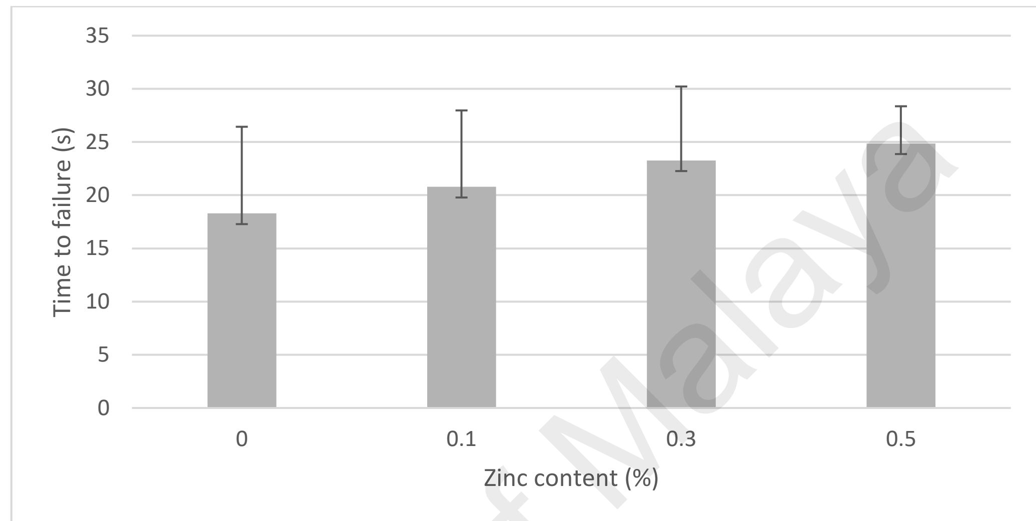

Figure 5.0.1: Comparison of time-to-failure of SAC305 alloy solders with incremental zinc content

University of Malaya

From the data, the trend for the TTF was found to be increasing TTF for lower Zn content:

$$0.5\%\ \text{Zn} \geq 0.3\%\ \text{Zn} > 0.1\%\ \text{Zn} \geq 0\%\ \text{Zn}$$

There was a ***12%*** difference between the TTF values of 0% Zn and 0.1% Zn samples, which was considered insignificant. Likewise, the ***6***% difference between the 0.3% and 0.5% samples was also considered insignificant thus the difference in time was considered to insignificant as well. However, the ***26***% difference in TTF between the 0% Zn and 0.5% Zn was considered significant and indicates that the ECM process experienced by the samples with a higher Zn content occurred at a slower rate than that those at a lower Zn content. This was in-line with findings by L Hua and Yang (2011)

and Tanaka (2002) who found that dendrite growth of undoped SAC solder was higher than that of SAC solder doped with Zn.

It was hypothesised that this may be the effect of intermetallic compound (IMC) formation on the surface of the substrate. The pure SAC305 sample would perhaps, in this case, contain Cu_6Sn_5, Cu_3Sn and/or Ag_3Sn (Nah et al., 2005) as the major IMCs, while the Zn-containing samples may have contained Cu_5Zn_8 and $CuZn_5$ IMCs (Chiu et al., 2002). However, as the studies by Nah and Chiu et al. are for experimental setups with a higher content of Zn, consideration must be given for the formation of other IMCs such as $ZnCl_2$, ZnO, $SnCl_2$, $Sn(OH)_4$ and so forth.

It is also possible that the formation of a Sn-Zn passive film may have suppressed the Zn dissolution reaction at the anode, thus prolonging the TTF. Tanaka (2002) hypothesised this in his study of Sn-9Zn corrosion, where the alloy was observed to undergo a period of inaction after exhibiting an initial dissolution reaction in the anode. With lower Sn content in the Zn-containing samples, the higher EMF and oxidation rate of Zn may have been countered by the rate of formation of the passive layer, thus leading to the delay in TTF.

As an overall, however, this indicates that the rate of corrosion and the rate of ECM cannot be conflated. Studies by J.-C. Liu et al. (2015) and L Hua and Yang (2011) both indicate that the addition of Zn to SAC alloys will result in an increase in the overall rate of corrosion, but such is not the case that has been observed here for electrochemical migration.

5.1.2 Hydrogen gas generation

In the duration of the water drop test, it was observed that the sample containing 0.3% and 5% Zn showed consistently lower current readings than the samples containing 0% and 0.1% Zn for most of the test. However, within the last 200 seconds of the test, much

University of Malaya

higher readings were observed for the 0.3% and 0.5% Zn samples that would occasionally exceed those of the 0% Zn sample.

This was attributed to the hydrogen generation reaction occurring at the cathode. To wit, two competing reactions occur at the cathode simultaneously (Zhong, Chen, et al., 2017):

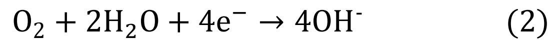

$$O_2 + 2H_2O + 4e^- \rightarrow 4OH^- \qquad (2)$$

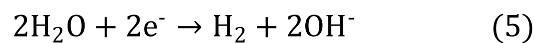

$$2H_2O + 2e^- \rightarrow H_2 + 2OH^- \qquad (5)$$

As the WD test involved placing a large droplet of water onto the surface of a sample, it can be hypothesised that the amount of dissolved and diffused oxygen within the water droplet is low due to the high electrolyte layer thickness, thus favouring reaction (5) over reaction (2). Throughout the experiment, it was observed that effervescence was ongoing in the full duration of the experiment.

It was observed, however, that the samples with higher Zn content had a more vigorous rate of effervescence than those with lower Zn content. This is in-line with the expectations from corrosion processes – Zn is located higher in the electrochemical series and thus would have a higher oxidation rate than Sn.

However, this vigorous generation of bubbles within the system would result in a higher convection, which may have led to the interference of the dendrite formation process, that bridges the cathode and anode. This was hypothesised to be the cause of the lower readings for the 0.3% and 0.5% samples.

As observed in Figure 5.0.2, the size and quantity of hydrogen bubbles between the four samples differed greatly: the undoped sample only had a few very large bubbles, the 0.1% Zn sample had a few very large bubbles, while the 0.3% Zn sample had a large quantity of very small bubbles. The 0.5% sample, on the other hand, was observed to

University of Malaya

have a large quantity of medium-sized bubbles. Two assumptions were made for this process: (a) That the only other competing gas-phase reaction within the system is reaction (2) and that the oxygen consumption rate far outstrips the oxygen diffusion rate into water; and (b) That larger bubbles are formed due to the coalescence of small bubbles.

In this case, the medium-sized bubbles of the 0.3% and 0.5% samples indicate a higher rate of effervescence than that of the 0% and 0.1% samples as the bubbles had already coalesced together. The combination of the higher effervescent rate and the larger bubbles was the cause of the interruption of the dendrite formation process, leading to the initial lower readings for the first half of the study.

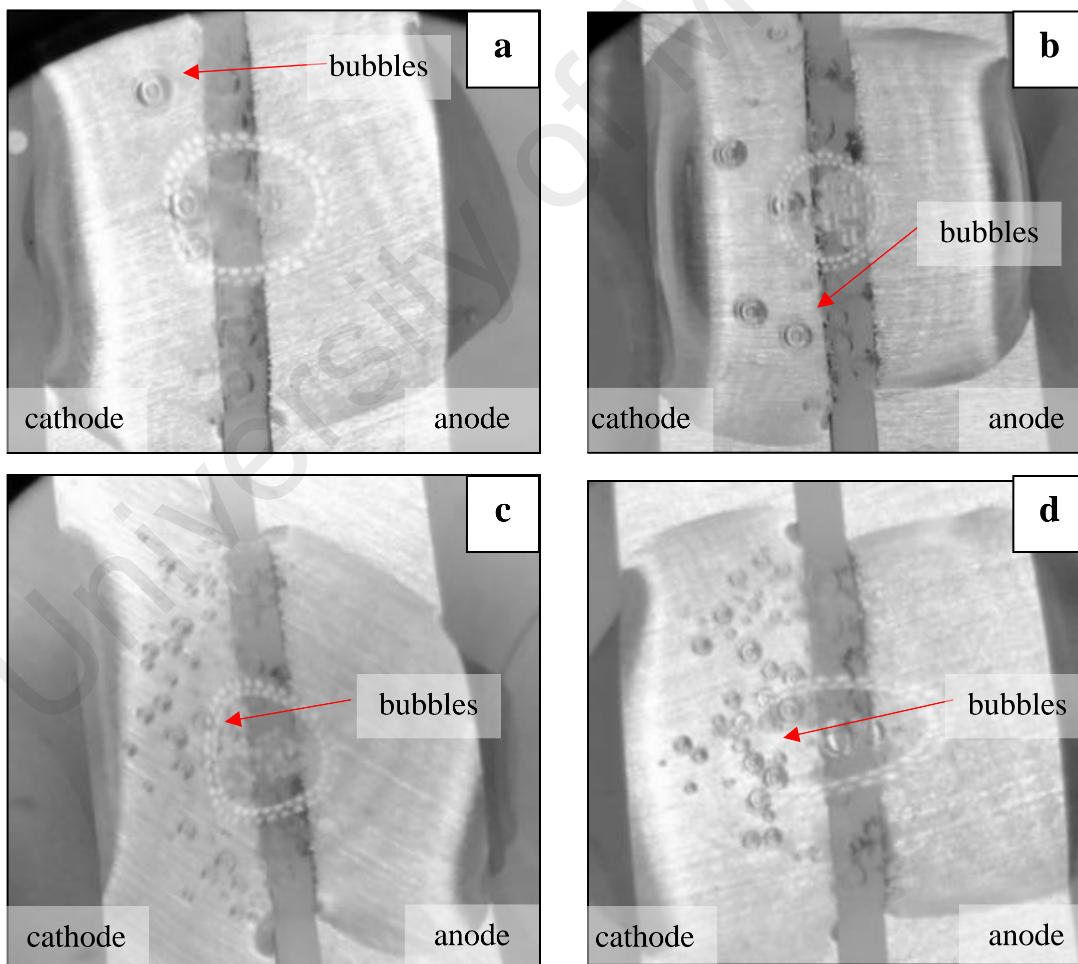

Figure 5.0.2: Effervescence formation observed at the 1 min mark for SAC305 alloys containing: (a) 0% Zn; (b) 0.1% Zn; (c) 0.3% Zn; (d) 0.5% Zn

University of Malaya

However, as the test proceeded, it was observed that the rate of effervescence gradually reduced, to a point where there was no discernible difference between all four samples due to the low rate of bubble generation, as well as the interference of precipitates for visual observation. Such was observed at the 6 min mark, as per Figure 5.0.3.

As the electrolyte layer thickness was also observed to have reduced during the progress of the experiment, it could be inferred that the combination of lower effervescence generation and the lower electrolyte thickness resulted in an overall rise in dendrite connections between the anode and the cathode. Likewise, as the rate of corrosion would be higher for samples with higher Zn content, this would lead to higher current readings in the last quarter of the WD test.

University of Malaya

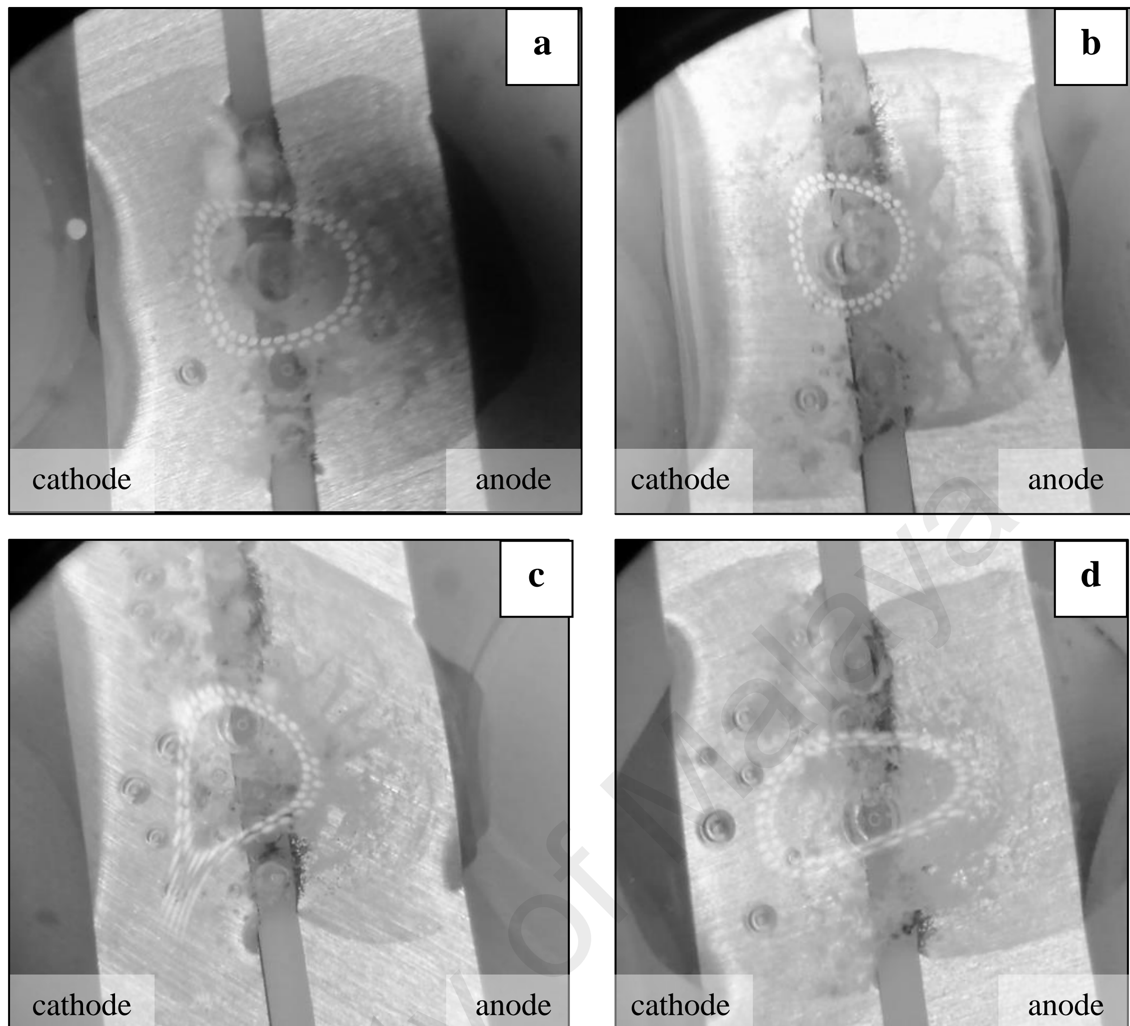

Figure 5.0.3: Effervescence formation observed at the 6 min mark for SAC305 alloys containing: (a) 0% Zn; (b) 0.1% Zn; (c) 0.3% Zn; (d) 0.5% Zn

5.2 Morphological analysis of ECM corrosion products

As previously mentioned in Section 5.1.2, the samples containing higher Zn content experienced a higher rate of reaction due to the higher position of Zn in the electrochemical series compared to Sn. This can be observed in

Figure 5.0.4, where the density of corrosion product (i.e. the white precipitate) drastically increases between the 0% and 0.5% Zn samples.

University of Malaya

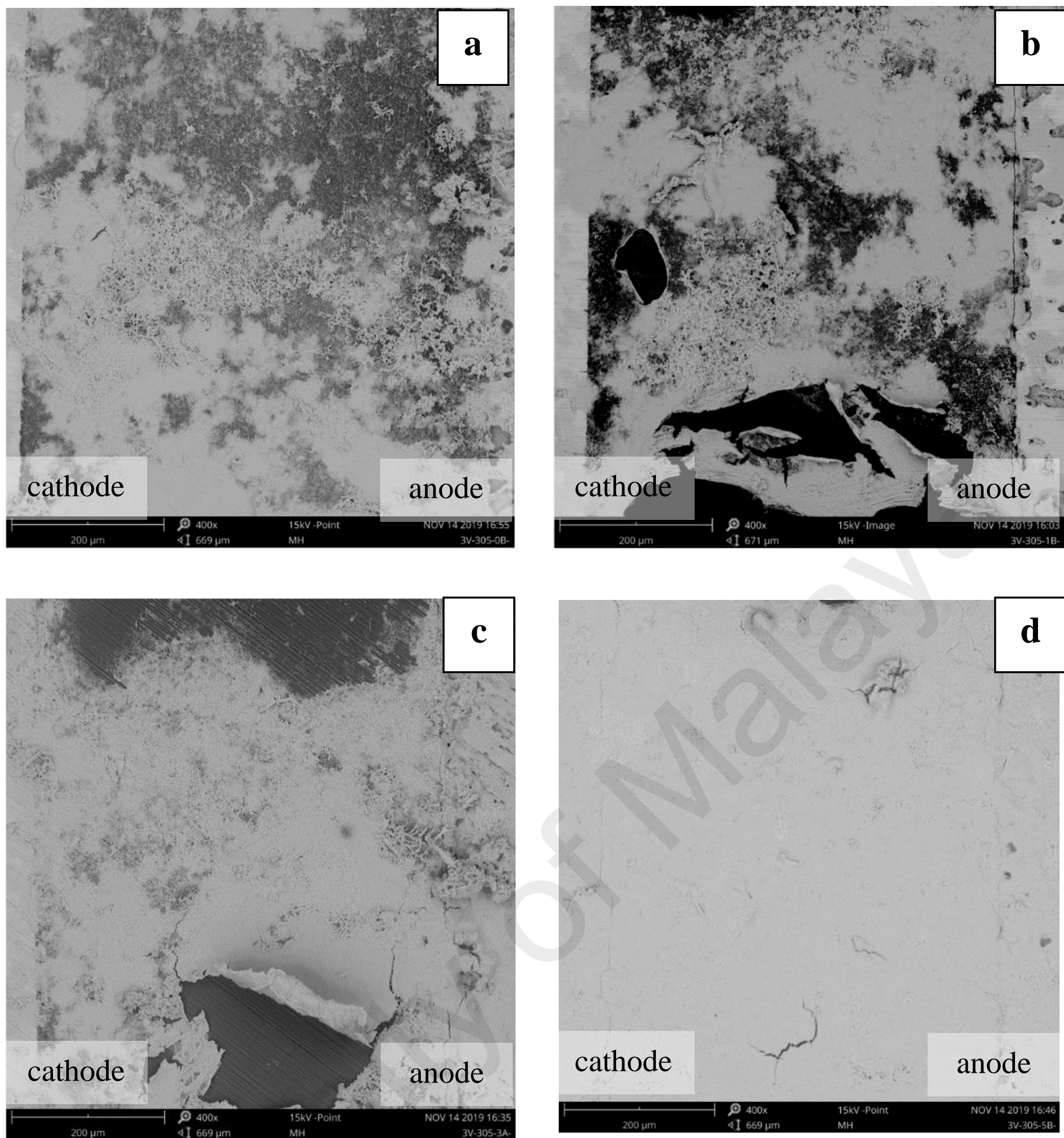

Figure 5.0.4: Comparison of sample surface at 400x magnification of SAC305 samples containing: (a) 0% Zn; (b) 0.1% Zn; (c) 0.3% Zn; (d) 0.5% Zn

University of Malaya

Furthermore, SEM images revealed a gradual change for the dendrite morphology upon an increase the amount of Zn contained within an SAC305 alloy. Undoped SAC305 samples were observed to be fern-shaped with thick spines and very sharp, diamond-shaped protrusions as pictured in

Figure 5.0.5. These appeared thick and angular with a heavy branching structure similar to tap-roots on plants. Adversely, the 0.5% Zn sample was observed to have very thin and needle-like dendrites, with no observable protrusions. It has a similar backbone-

like branching structure for its dendrite growth, but the observed branches were overall finer and similar to a fibrous-root structure.

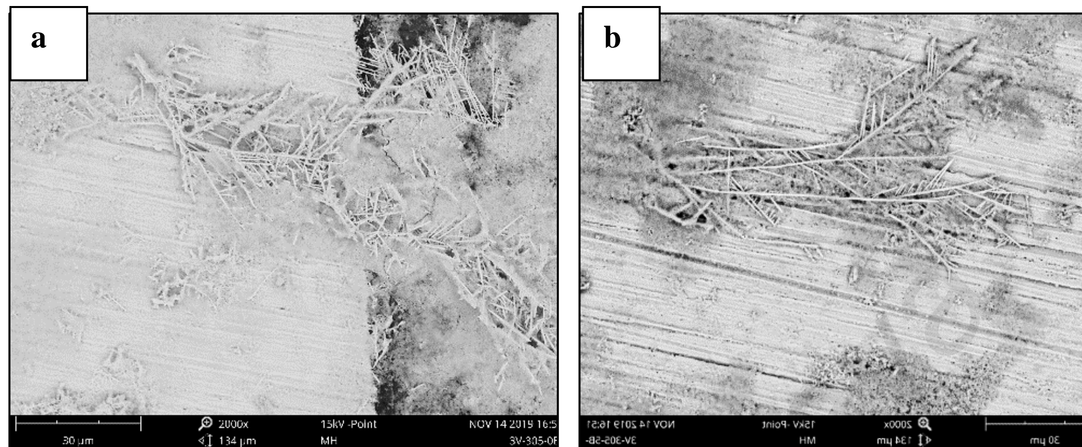

Figure 5.0.5: SE micrographs of the dendrite topography for SAC305 (left side) and SAC305 + 0.5% Zn (right side) at: 2000x magnification

A closer comparison of the samples yielded the hypothesis that the angular crystalline structure on the formed dendrites of undoped SAC305 was Sn as there was a gradual reduction of the degree of formation of these crystals in the 0.1% Zn sample before it disappeared entirely in the 0.5% Zn sample. This would indicate that a higher Sn content would lead to a higher concentration of Sn ions in the dendrite formation. Similar observations were made by Li Hua et al. (2011) who had found “cactus-like” structures which were similar to the angular shapes found in this study.

This phenomenon could help explain the lower TTF results of the 0% sample: A more angular structure would provide a higher surface area for nucleation of dendrite formation. It could thus be hypothesised that this would accelerate the growth of the dendrite cluster, leading to a low TTF.

However, the nature of Zn that is more easily oxidised compared to Sn may also be the reason of the morphology shift as pictured in Figure 5.0.6. Upon increasing fraction

University of Malaya

of Zn within the alloy, the dendrites grow finer and lose their angular “cactus”-like look, which would support the hypothesis that the angular shapes at the tips were primarily Sn in nature. As the Zn content of these alloys were still relatively low, the dendrites still maintained similarities to the dendrite morphology of undoped SAC (e.g. the thick backbone structure) but the differences in morphology is unmistakeable with higher Zn content.

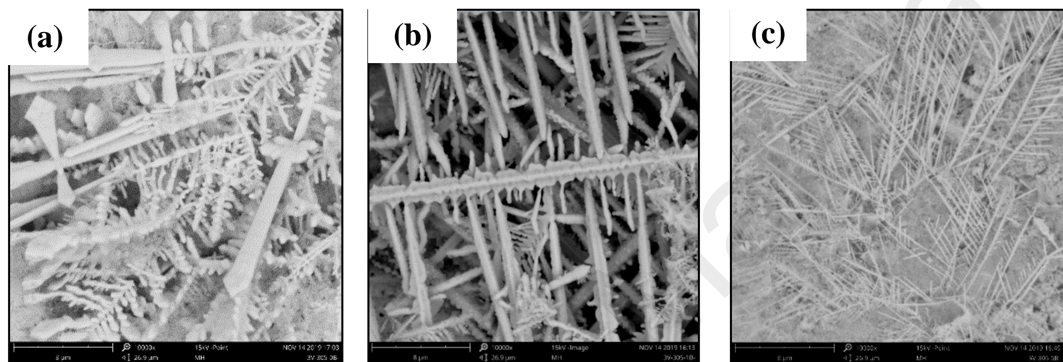

Figure 5.0.6: SE micrographs of dendrite morphology at 10,000x magnifictation for: (a) SAC305; (b) SAC305 + 0.1% Zn; (c) SAC305 + 0.5% Zn

Another observation can be made about the nature of the 0% and 0.1% Zn samples. Pictured in Figure 5.0.7, the secondary dendrites were observed to be longer compared to those of the 0.3% and 0.5% Zn sample. It was discussed by Minzari et al. (2011) that dendrites with a longer shape would have shorter time-to-failure as the distance between the cathode and the dendrite would be lower. This may well be the reason behind the early failure of the 0% and 0.1% samples. An early development of longer dendrites compared to the other samples would result in an earlier time to failure.

University of Malaya

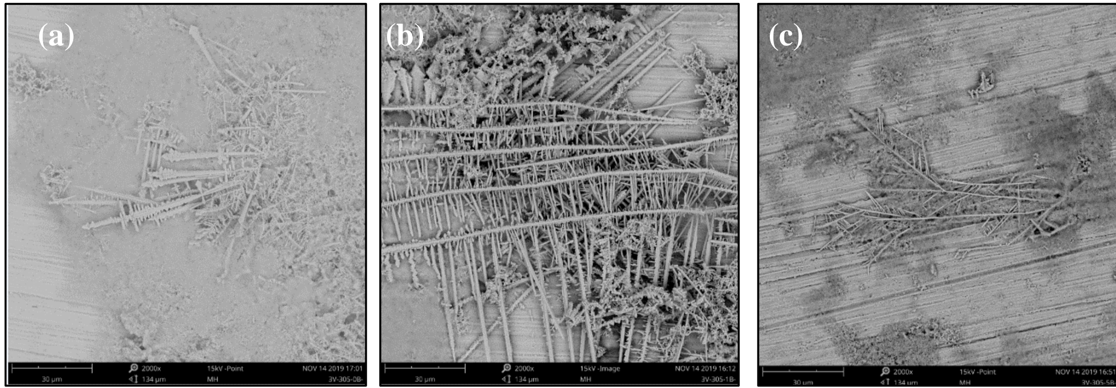

Figure 5.0.7: Macrostructure of dendrites for SAC alloys containing: (a) 0% Zn; (b) 0.1% Zn; (c) 0.5% Zn

To confirm these hypotheses, it is imperative that energy dispersive X-ray analysis (EDX) be conducted on the samples to further understand the elemental breakdown of the dendrites.

University of Malaya

6.0 CONCLUSIONS AND RECOMMENDATIONS

6.1 Conclusions

The following conclusions could be drawn from the study:

1. The incorporation of Zn into SAC solder alloys increases the time-to-failure of SAC305 solder alloys. This was hypothesised to be the result of IMC formation and Sn-Zn passivation that resulted in a longer time to short circuit.
2. A higher Zn content in SAC305 results in a change of the dendrite morphology. Dendrites will become finer and more needle-like, while exhibiting more fibrous root-like behaviour in its growth structure.

6.2 Recommendations for future works

This test study was not able to accurately identify the exact chemical composition of the dendrites due to lack of information. It is thus highly recommended that a test such as EDX be conducted to further understand the effects of Zn on the dendrite formation. Furthermore, it is highly recommended that a quantitative test such as the electrochemical impedance spectroscopy (EIS) be conducted to give a more reliable output and holistic view of the corrosion process of these alloys that proceed alongside the ECM process. As the ECM system is capable of being affected by issues like high effervescence affecting the dendrite formation process, a concurrent test that is more gradual and less destructive may offer insight into the long-term feasibility of these studies.

Alternatively, to further study higher Zn content in Sn-3.0Ag-0.5Cu solder alloys using the water drop test method, it would be advisable to run tests under a lower voltage or a lower concentration of electrolyte ions to minimise the interference of hydrogen effervescence on the circuit. Furthermore, solder alloy sample polishing should be done

University of Malaya

entirely by machine to minimise the probability of voids and protrusions on the substrate surface that may act as weak points in the system.

University of Malaya

REFERENCES

Andersson, C., & Liu, J. (2008). Effect of corrosion on the low cycle fatigue behavior of Sn–4.0 Ag–0.5 Cu lead-free solder joints. *International Journal of Fatigue, 30*(5), 917-930.

Bockris, J. O. M., & Reddy, A. K. (1970). *Modern electrochemistry: an introduction to an interdisciplinary area [by] John O'M. Bockris and Amulya KN Reddy* (Vol. 2): Plenum Publishing Corporation.

Chang, T.-C., Hon, M.-H., Wang, M.-C., & Lin, D.-Y. (2004). Electrochemical behaviors of the Sn-9Zn-xAg lead-free solders in a 3.5 wt% NaCl solution. *Journal of The Electrochemical Society, 151*(7), C484-C491.

Che, F., Luan, J., & Baraton, X. (2008). *Effect of silver content and nickel dopant on mechanical properties of Sn-Ag-based solders.* Paper presented at the 2008 58th Electronic Components and Technology Conference.

Che, F., Poh, E. C., Zhu, W., & Xiong, B. (2007). *Ag content effect on mechanical properties of Sn-xAg-0.5 Cu solders.* Paper presented at the 2007 9th Electronics Packaging Technology Conference.

Chiu, M., Wang, S., & Chuang, T. (2002). Intermetallic compounds formed during interfacial reactions between liquid Sn-8Zn-3Bi solders and Ni substrates. *Journal of electronic materials, 31*(5), 494-499.

Cho, M. G., Kang, S. K., Shih, D.-Y., & Lee, H. M. (2007). Effects of minor additions of Zn on interfacial reactions of Sn-Ag-Cu and Sn-Cu solders with various Cu substrates during thermal aging. *Journal of electronic materials, 36*(11), 1501-1509.

Choi, J.-W., Cha, H.-S., & Oh, T.-S. (2002). Mechanical properties and shear strength of Sn-3.5 Ag-Bi solder alloys. *Materials transactions, 43*(8), 1864-1867.

Dominkovics, C., & Harsanyi, G. (2008). Fractal description of dendrite growth during electrochemical migration. *Microelectronics Reliability, 48*(10), 1628-1634.

Dušek, M., Szendiuch, I., Bulva, J., & Zelinka, M. (2016). Wettability–SnPb and Lead-free.

Efzan Mhd Noor, E., & Singh, A. (2014). Review on the effect of alloying element and nanoparticle additions on the properties of Sn-Ag-Cu solder alloys. *Soldering & Surface Mount Technology, 26*(3), 147-161.

El-Daly, A., Hammad, A., Fawzy, A., & Nasrallh, D. (2013). Microstructure, mechanical properties, and deformation behavior of Sn–1.0 Ag–0.5 Cu solder after Ni and Sb additions. *Materials & Design, 43*, 40-49.

El-Daly, A., Swilem, Y., Makled, M., El-Shaarawy, M., & Abdraboh, A. (2009). Thermal and mechanical properties of Sn–Zn–Bi lead-free solder alloys. *Journal of Alloys and Compounds, 484*(1-2), 134-142.

Fayeka, M., Haseeb, A., & Fazal, M. (2017). Electrochemical corrosion behaviour of Pb-free SAC 105 and SAC 305 solder alloys: a comparative study. *Sains Malaysiana, 46*(2), 295-302.

Fukami, K., Nakanishi, S., Yamasaki, H., Tada, T., Sonoda, K., Kamikawa, N., . . . Nakato, Y. (2007). General mechanism for the synchronization of electrochemical oscillations and self-organized dendrite electrodeposition of metals with ordered 2D and 3D microstructures. *The Journal of Physical Chemistry C, 111*(3), 1150-1160.

George, E., & Pecht, M. (2016). RoHS compliance in safety and reliability critical electronics. *Microelectronics Reliability, 65*, 1-7.

Hassam, S., Dichi, E., & Legendre, B. (1998). Experimental equilibrium phase diagram of the Ag–Bi–Sn system. *Journal of Alloys and Compounds, 268*(1-2), 199-206.

He, X., Azarian, M. H., & Pecht, M. G. (2014). Analysis of the kinetics of electrochemical migration on printed circuit boards using Nernst-Planck transport equation. *Electrochimica Acta, 142*, 1-10.

Henshall, G., Bath, J., Sethuraman, S., Geiger, D., Syed, A., Lee, M., . . . Xie, W. (2009). Comparison of thermal fatigue performance of SAC105 (Sn-1.0 Ag-0.5 Cu), Sn-3.5 Ag,

University of Malaya

and SAC305 (Sn-3.0 Ag-0.5 Cu) BGA components with SAC305 solder paste. *Proceedings of IPC APEX*.

Hua, L., Hou, H., Zhang, H., Wu, T., & Deng, Y. (2010). *Effects of Zn, Ge doping on electrochemical migration, oxidation characteristics and corrosion behavior of lead-free Sn-3.0 Ag-0.5 Cu solder for electronic packaging*. Paper presented at the 2010 11th International Conference on Electronic Packaging Technology & High Density Packaging.

Hua, L., Sou, M. W., Zhang, W. J., & Hu, Q. (2011). *Electrochemical migration and rapid whisker growth of Zn and Bi dopings in Sn-3.0 Ag-0.5 Cu solder in 3wt.% NaCl solution.* Paper presented at the Advanced Materials Research.

Hua, L., & Yang, C. (2011). Corrosion behavior, whisker growth, and electrochemical migration of Sn–3.0 Ag–0.5 Cu solder doping with In and Zn in NaCl solution. *Microelectronics Reliability, 51*(12), 2274-2283.

Jiang, S., Liao, B., Chen, Z., & Guo, X. (2018). Investigation of Electrochemical Migration of Tin and Tin-Based Lead-Free Solder Alloys under Chloride-Containing Thin Electrolyte Layers. *INTERNATIONAL JOURNAL OF ELECTROCHEMICAL SCIENCE, 13*(10), 9942-9949.

Jung, J.-Y., Lee, S.-B., Joo, Y.-C., Lee, H.-Y., & Park, Y.-B. (2008). Anodic dissolution characteristics and electrochemical migration lifetimes of Sn solder in NaCl and Na2SO4 solutions. *Microelectronic Engineering, 85*(7), 1597-1602.

Jung, J.-Y., Lee, S.-B., Lee, H.-Y., Joo, Y.-C., & Park, Y.-B. (2008). Effect of ionization characteristics on electrochemical migration lifetimes of Sn-3.0 Ag-0.5 Cu solder in NaCl and Na 2 SO 4 solutions. *Journal of electronic materials, 37*(8), 1111-1118.

Kanlayasiri, K., & Meesathien, N. (2018). Effects of Zinc Oxide Nanoparticles on Properties of SAC0307 Lead-Free Solder Paste. *Advances in Materials Science and Engineering, 2018*.

Kotadia, H., Mokhtari, O., Clode, M., Green, M., & Mannan, S. (2012). Intermetallic compound growth suppression at high temperature in SAC solders with Zn addition on Cu and Ni–P substrates. *Journal of Alloys and Compounds, 511*(1), 176-188.

Lee, S., & Staehle, R. (1997). Adsorption studies of water on copper, nickel, and iron using the quartz-crystal microbalance technique: Assessment of BET and FHH models of adsorption. *Materials and Corrosion, 48*(2), 86-94.

Li, D., Conway, P. P., & Liu, C. (2008). Corrosion characterization of tin–lead and lead free solders in 3.5 wt.% NaCl solution. *Corrosion Science, 50*(4), 995-1004.

Li, J., Mannan, S., Clode, M., Johnston, C., & Crossley, A. (2007). Dissolution and interfacial reaction of Nb in contact with the molten 52In–48Sn solder. *Acta Materialia, 55*(15), 5057-5071.

Lin, H.-J., & Chuang, T.-H. (2010). Effects of Ce and Zn additions on the microstructure and mechanical properties of Sn–3Ag–0.5 Cu solder joints. *Journal of Alloys and Compounds, 500*(2), 167-174.

Liu, J.-C., Park, S., Nagao, S., Nogi, M., Koga, H., Ma, J.-S., . . . Suganuma, K. (2015). The role of Zn precipitates and Cl− anions in pitting corrosion of Sn–Zn solder alloys. *Corrosion Science, 92*, 263-271.

Liu, W., & Lee, N.-C. (2007). The effects of additives to SnAgCu alloys on microstructure and drop impact reliability of solder joints. *Jom, 59*(7), 26-31.

Liu, Y., Sun, F., & Li, X. (2014). Effect of Ni, Bi concentration on the microstructure and shear behavior of low-Ag SAC–Bi–Ni/Cu solder joints. *Journal of Materials Science: Materials in Electronics, 25*(6), 2627-2633.

Lloyd, J., Murray, C., Ponoth, S., Cohen, S., & Liniger, E. (2006). The effect of Cu diffusion on the TDDB behavior in a low-k interlevel dielectrics. *Microelectronics Reliability, 46*(9-11), 1643-1647.

Mahdavifard, M. H., Sabri, M. F. M., Shnawah, D. A., Said, S., Badruddin, I. A., & Rozali, S. (2015). The effect of iron and bismuth addition on the microstructural, mechanical, and thermal properties of Sn–1Ag–0.5 Cu solder alloy. *Microelectronics Reliability, 55*(9-10), 1886-1890.

Medgyes, B., Horváth, B., Illés, B., Shinohara, T., Tahara, A., Harsányi, G., & Krammer, O. (2015). Microstructure and elemental composition of electrochemically formed

University of Malaya

dendrites on lead-free micro-alloyed low Ag solder alloys used in electronics. *Corrosion Science, 92*, 43-47.
Minzari, D., Jellesen, M. S., Møller, P., & Ambat, R. (2011). On the electrochemical migration mechanism of tin in electronics. *Corrosion Science, 53*(10), 3366-3379.
Mohanty, U. S., & Lin, K.-L. (2006). Effect of Al on the electrochemical corrosion behaviour of Pb free Sn–8.5 Zn–0.5 Ag–XAl–0.5 Ga solder in 3.5% NaCl solution. *Applied surface science, 252*(16), 5907-5916.
Nah, J., Suh, J., & Tu, K. (2005). Effect of current crowding and Joule heating on electromigration-induced failure in flip chip composite solder joints tested at room temperature. *Journal of applied physics, 98*(1), 013715.
Nazeri, M. F. M., & Mohamad, A. A. (2014). Corrosion measurement of Sn–Zn lead-free solders in 6 M KOH solution. *Measurement, 47*, 820-826.
Nishikata, A., Ichihara, Y., Hayashi, Y., & Tsuru, T. (1997). Influence of electrolyte layer thickness and pH on the initial stage of the atmospheric corrosion of iron. *Journal of The Electrochemical Society, 144*(4), 1244-1252.
Noh, B.-I., Yoon, J.-W., Hong, W.-S., & Jung, S.-B. (2009). Evaluation of electrochemical migration on flexible printed circuit boards with different surface finishes. *Journal of electronic materials, 38*(6), 902-907.
Nurul Liyana, K. (2018). *Effects of Zn and A1 on corrosion characteristics of Sn-1.0 Ag-0.5 Cu alloys/Nurul Liyana Kamaruzaman.* University of Malaya,
Puechagut, C., Laügt, A.-M., Guéné, E., & Anisko, R. (2015). *Solder paste residue corrosivity assessment: Bono test.* Paper presented at the 2015 European Microelectronics Packaging Conference (EMPC).
Puttlitz, K. J., & Stalter, K. A. (2004). *Handbook of lead-free solder technology for microelectronic assemblies*: CRC Press.
Rice, D., Cappell, R., Phipps, P., & Peterson, P. (1982). Indoor atmospheric corrosion of copper, nickel, cobalt, and iron, in atmospheric corrosion, ed. WH Ailor. In: Wiley, New York.
Sabri, M. F. M., Shnawah, D. A., Badruddin, I. A., Said, S. B. M., Che, F. X., & Ariga, T. (2013). Microstructural stability of Sn–1Ag–0.5 Cu–xAl (x= 1, 1.5, and 2 wt.%) solder alloys and the effects of high-temperature aging on their mechanical properties. *Materials Characterization, 78*, 129-143.
Sarveswaran, C., Salleh, E. M., Jalar, A., Samsudin, Z., Ali, M. Y. T., Ani, F. C., & Othman, N. K. (2017). *Investigation of corrosion on SAC 305, SAC 0307 and SAC 0307-0.03 P-0.005 Ni solder paste alloys in simulated body fluid (SBF).* Paper presented at the AIP Conference Proceedings.
Schwartz, M. M. (2014). *Soldering: Understanding the Basics*: ASM International.
Shyu, J. (1983). ROUGHNESS EVOLUTION AND DENDRITIC GROWTH IN ELECTRODEPOSITION.
Simillion, H., Van den Steen, N., Terryn, H., & Deconinck, J. (2016). Geometry influence on corrosion in dynamic thin film electrolytes. *Electrochimica Acta, 209*, 149-158.
Smith, D. R., Siewert, T. A., Stephen, L., & Madeni, J. C. (2002). *Database for solder properties with emphasis on new lead-free solders*. Retrieved from
Steppan, J., Roth, J., Hall, L., Jeannotte, D., & Carbone, S. (1987). A review of corrosion failure mechanisms during accelerated tests electrolytic metal migration. *Journal of The Electrochemical Society, 134*(1), 175-190.
Sun, M., Liao, H.-G., Niu, K., & Zheng, H. (2013). Structural and morphological evolution of lead dendrites during electrochemical migration. *Scientific reports, 3*, 3227.
Sungkhaphaitoon, P., & Chantaramanee, S. (2018). Effects of Indium Content on Microstructural, Mechanical Properties and Melting Temperature of SAC305 Solder Alloys. *Russian Journal of Non-Ferrous Metals, 59*(4), 385-392.
Takemoto, T., Latanision, R., Eagar, T., & Matsunawa, A. J. C. S. (1997). Electrochemical migration tests of solder alloys in pure water. *39*(8), 1415-1430.
Tanaka, H. (2002). Factors leading to ionic migration in lead-free solder. *Espec technology report*(14).

University of Malaya

Tsao, L., Chang, S., Lee, C., Sun, W., & Huang, C. (2010). Effects of nano-Al2O3 additions on microstructure development and hardness of Sn3. 5Ag0. 5Cu solder. *Materials & Design, 31*(10), 4831-4835.

Wang, F., Ma, X., & Qian, Y. (2005). Improvement of microstructure and interface structure of eutectic Sn–0.7 Cu solder with small amount of Zn addition. *Scripta materialia, 53*(6), 699-702.

Wang, J.-X., Xue, S.-B., Han, Z.-J., Yu, S.-L., Chen, Y., Shi, Y.-P., & Wang, H. (2009). Effects of rare earth Ce on microstructures, solderability of Sn–Ag–Cu and Sn–Cu–Ni solders as well as mechanical properties of soldered joints. *Journal of Alloys and Compounds, 467*(1-2), 219-226.

Wang, Y., Chang, C., & Kao, C. (2009). Minimum effective Ni addition to SnAgCu solders for retarding Cu3Sn growth. *Journal of Alloys and Compounds, 478*(1-2), L1-L4.

Warren, G. W., Wynblatt, P., & Zamanzadeh, M. (1989). The role of electrochemical migration and moisture adsorption on the reliability of metallized ceramic substrates. *Journal of electronic materials, 18*(2), 339-353.

Wu, B., Chan, Y., Alam, M., & Jillek, W. (2006). Electrochemical corrosion study of Pb-free solders. *Journal of materials research, 21*(1), 62-70.

Xu, J., Liu, X., Li, X., Barbero, E., & Dong, C. (2006). Effect of Sn concentration on the corrosion resistance of Pb-Sn alloys in H2SO4 solution. *Journal of power sources, 155*(2), 420-427.

Yakymovych, A., Švec, P., Orovcik, L., Bajana, O., & Ipser, H. (2018). Nanocomposite SAC solders: the effect of adding Ni and Ni-Sn nanoparticles on morphology and mechanical properties of Sn-3.0 Ag-0.5 Cu solders. *Journal of electronic materials, 47*(1), 117-123.

Yamamoto, T., & Tsubone, K.-i. (2007). Assembly technology using lead-free solder. *Fujitsu scientific and technical journal, 43*(1), 50-58.

Yi, P., Dong, C., Ji, Y., Yin, Y., Yao, J., & Xiao, K. (2019). Electrochemical migration failure mechanism and dendrite composition characteristics of Sn96. 5Ag3. 0Cu0. 5 alloy in thin electrolyte films. *Journal of Materials Science: Materials in Electronics, 30*(7), 6575-6582.

Yu, D., Jillek, W., & Schmitt, E. (2006). Electrochemical migration of lead free solder joints. *Journal of Materials Science: Materials in Electronics, 17*(3), 229-241.

Zhang, L., Xue, S. B., Zeng, G., Gao, L. L., & Ye, H. (2012). Interface reaction between SnAgCu/SnAgCuCe solders and Cu substrate subjected to thermal cycling and isothermal aging. *Journal of Alloys and Compounds, 510*(1), 38-45.

Zhong, X., Chen, L., Medgyes, B., Zhang, Z., Gao, S., & Jakab, L. J. R. A. (2017). Electrochemical migration of Sn and Sn solder alloys: a review. *7*(45), 28186-28206.

Zhong, X., Guo, X., Qiu, Y., Chen, Z., & Zhang, G. (2013). In situ study the electrochemical migration of tin under unipolar square wave electric field. *Journal of The Electrochemical Society, 160*(11), D495-D500.

Zhong, X., Yu, S., Chen, L., Hu, J., & Zhang, Z. J. J. o. M. S. M. i. E. (2017). Test methods for electrochemical migration: a review. *28*(2), 2279-2289.

Zhong, X., Zhang, G., & Guo, X. (2015). The effect of electrolyte layer thickness on electrochemical migration of tin. *Corrosion Science, 96*, 1-5.

Zhong, X., Zhang, G., Qiu, Y., Chen, Z., & Guo, X. (2013). Electrochemical migration of tin in thin electrolyte layer containing chloride ions. *Corrosion Science, 74*, 71-82.

University of Malaya